CONTRACT NO.: DAMD17-88-Z-8008

TITLE: FUNDAMENTAL STUDIES IN THE MOLECULAR BASIS OF LASER INDUCED RETINAL DAMAGE

PRINCIPAL INVESTIGATOR: AARON LEWIS

PI ADDRESS: Hadassah Laser Center
Hebrew University-Hadassah Hospital
Ein Kerem
Jerusalem, Israel

REPORT DATE: December 30, 1989

TYPE OF REPORT: Midterm

PREPARED FOR: U.S. ARMY MEDICAL RESEARCH AND DEVELOPMENT COMMAND
FORT DETRICK
FREDERICK, MARYLAND 21701-5012

DISTRIBUTION STATEMENT: Approved for public release;
distribution unlimited

The findings in this report are not to be construed as an official Department of the Army position unless so designated by other authorized documents.

SECURITY CLASSIFICATION OF THIS PAGE

REPORT DOCUMENTATION PAGE

Form Approved
OMB No. 0704-0188

1a. REPORT SECURITY CLASSIFICATION Unclassified	1b. RESTRICTIVE MARKINGS
2a. SECURITY CLASSIFICATION AUTHORITY	3 DISTRIBUTION / AVAILABILITY OF REPORT Approved for public release; distribution unlimited
2b. DECLASSIFICATION / DOWNGRADING SCHEDULE	
4. PERFORMING ORGANIZATION REPORT NUMBER(S)	5. MONITORING ORGANIZATION REPORT NUMBER(S)
6a. NAME OF PERFORMING ORGANIZATION Hadassah Laser Center 6b. OFFICE SYMBOL (If applicable)	7a. NAME OF MONITORING ORGANIZATION
6c. ADDRESS (City, State, and ZIP Code) Hebrew University-Hadassah Hospital Ein Kerem Jerusalem, Israel	7b. ADDRESS (City, State, and ZIP Code)
8a. NAME OF FUNDING / SPONSORING ORGANIZATION U.S. Army Medical Research & Development Command 8b. OFFICE SYMBOL (If applicable)	9. PROCUREMENT INSTRUMENT IDENTIFICATION NUMBER DAMD17-88-Z-8008
8c. ADDRESS (City, State, and ZIP Code) Fort Detrick Frederick, Maryland 21701-5012	10. SOURCE OF FUNDING NUMBERS PROGRAM ELEMENT NO. 62787A; PROJECT NO 3M1-62787A878; TASK NO. BA; WORK UNIT ACCESSION NO. WUDA314047

11. TITLE (Include Security Classification)
(U) Fundamental Studies in the Molecular Basis of Laser Induced Retinal Damage

12. PERSONAL AUTHOR(S)
Aaron Lewis

13a. TYPE OF REPORT	13b. TIME COVERED	14. DATE OF REPORT (Year, Month, Day)	15. PAGE COUNT
Midterm	FROM 11/1/87 TO 4/30/89	1989 December 30	61

16. SUPPLEMENTARY NOTATION

17. COSATI CODES			18. SUBJECT TERMS (Continue on reverse if necessary and identify by block number)
FIELD	GROUP	SUB-GROUP	~~RA 3~~; Lab Animals; Turtles; Frogs; Safety Levels; LASERS; Visual Sensitivity, RETINAL DAMAGE
09	03		
06	04		

19. ABSTRACT (Continue on reverse if necessary and identify by block number)

The January 1988 issue of **Physics Today** featured our work on the biophysics of visual photoreception. In this work we investigated the absorption of a single photon by a pigment molecule called rhodopsin in a photoreceptor cell in the retina. The retina is where the excitation of visual sensation begins, where single photons are amplified, where the eye adapts to light levels and generates a partially processed signal to the brain. Except for the partial processing of the image, these functions of the retina occur largely in a cell called the photoreceptor, which absorbs and amplifies the photon and transduces it to a neural response.

We also explored the absorption and surface-enhanced Raman spectra of mono-layers of retinal and styryl pyridinium dyes were obtained. The results have yielded new information on the absorption properties of these highly polarizable molecules. Information on the structure of the monolayer films have been deduced from the vibrational spectra. Enhancement

20. DISTRIBUTION / AVAILABILITY OF ABSTRACT ☐ UNCLASSIFIED/UNLIMITED ☒ SAME AS RPT. ☐ DTIC USERS	21 ABSTRACT SECURITY CLASSIFICATION Unclassified
22a. NAME OF RESPONSIBLE INDIVIDUAL Mary Frances Bostian	22b TELEPHONE (Include Area Code) 301-663-7325 22c. OFFICE SYMBOL SGRD-RMI-S

DD Form 1473, JUN 86 *Previous editions are obsolete.* SECURITY CLASSIFICATION OF THIS PAGE

19. Abstract (continued)

mechanisms have been characterized and vibrational assignments have been made for the surface-enhanced Raman spectra of these monolayers.

A study on the second harmonic signal from monolayers of retinal and retinal Schiff bases was reported. The results have yielded information on the monolayer structure and demonstrated that retinal and retinal Schiff bases have large second-order molecular hyperpolarizabilities with values of 1.4×10^{-28}, 1.2×10^{-28}, and 2.3×10^{-28} for retinal, the unprotonated Schiff base, and the protonated Schiff base, respectively. These values compare well with the known variation in the alteration in the dipole moment of such chromophores upon excitation.

In addition, optical imaging with resolution exceeding the diffraction limit with near-field scanning optical microscopy (NSOM) was demonstrated. The concept behind the technique and its experimental implementation was discussed. Images were presented which attested to its reproducibility and super-resolution capabilities. Although distinct, NSOM has technical features in common with scanning tunneling microscopy. However, since it is optically based it also shares many of the advantages of conventional optical microscopy, including non-destructiveness, speed, flexibility, and the ability to generate contrast in numerous ways.

FOREWORD

Opinions, interpretations, conclusions and recommendations are those of the author and are not necessarily endorsed by the U. S. Army.

✓ Where copyrighted material is quoted permission has been obtained to use such material.

✓ Where material from documents designated for limited distribution is quoted, permission has been obtained to use the material.

✓ Citations of commercial organizations and trade names in this report do not constitute an official Department of the Army endorsement or approval of the products or services of these organizations.

Aaron Lewis June 89

PI Signature Date

ABSORPTION AND VIBRATIONAL SPECTRA OF RETINAL AND RELATED MOLECULES WITH LARGE-INDUCED DIPOLES

Abstract

Absorption and surface-enhanced Raman spectra of retinal and styryl pyridinium dyes were obtained. The results have yielded new information on the absorption properties of these highly polarizable molecules. Information on the structure of the mo olayer films have been deduced from the vibrational spectra. Enhancement mechanisms have been characterized and vibrational assignments have been made for the recorded surface-enhanced Raman spectra.

1. Introduction

Molecules that undergo large light-induced changes in dipole are important in biology. These molecules occur naturally in a variety of biological systems. An important example of such a molecule is the retinal chromophore that is involved in visual excitation(1). Artificially synthesized compounds with large light-induced dipolar alterations have also played an important role in biophysical research. A group of such compounds are the styryl pyridinium dyes that have been very successfully employed to detect electrochromic alterations in membrane potential(2). In this paper we consider the surface properties of retinal and styryl pyridinium dyes by investigating the absorption and vibrational spectra of monolayers of these compounds deposited on silver island films and in certain instances directly on a glass surface. The chemical structures of these molecules are shown in Figure 1.

To investigate the spectra of monolayers we have employed the standard methodology of producing such thin films using Langmuir Blodgett techniques. This approach can in principle allow the investigation of the optical properties of these molecules without the effect of solvents that have a dominating effect on the spectral characteristics of such molecular species. The results we have obtained have yielded interesting insights into excited and ground state stabilization of the retinal versus the styryl pyridinium dyes and these results are correlated with the observed vibrational spectra. In addition the results indicate the effect of field induced enhancement of the Raman scattering cross sections when silver island films are employed.

2. Experimental Procedures

The silver island films used in the experiment were evaporated at ~1Å/sec at 300°K on to clean glass substrates in a Varian electron-beam evaporation system with base pressure of ~3×10^{-7}torr. An Inficon quartz crystal thickness monitor was used to measure the mass thickness of the deposited films.

The deposition scheme of monomolecular layers on a solid substrate (3) that we have used is very simple. First, the substrate is attached to a dipping head which employes a micrometer translator driven by a d.c. motor. After the substrate is immersed into a pure water subphase at 22°C with pH 6.5, the molecules are spread and compressed to set up a stable monolayer which is held in the complete condensation region. The substrate is then raised through the film at a deposition speed of 75 μm/sec. During the film transfer period, the decreasing area of the monolayer on the water subphase is also recorded to estimate the deposition ratio and the surface density of the molecules on the substrate. With this method a monolayer of good optical quality has been reproducibly deposited onto the surfaces of a native hydrophilic glass and a hydrophobic silver-island film.

Absorption spectra of the silver-island films and monolayers which had been deposited on quartz substrates, were obtained on a Cary 219 dual-beam spectrophotometer. The scattering and absorption induced by the substrates were corrected by putting an identical quartz plate in one of the exciting beams.

Raman scattering was excited by the argon laser lines, focused to a dimension of 2mm x 0.4mm line image on the sample plane at an angle of incidence of 45° with respect to the surface normal. The polarization of the laser was perpendicular to the incident planes in order to excite the long wavelength surface plasmons of the silver island films effectively(4). An argon ion laser with a power of less than 5mW was used. The scattered radiation was collected by an ellipsoidal mirror (5). A Spex 1877 Triplemate spectrometer was used to filter the Rayleigh scattered light, and to disperse the Raman scattering photons across the photocathode of a cooled intensified silicon photodiode array (EG&G PARC 1420) detector. The on-target integration time of the detector for each data scan was adjusted to be 3.2sec such that the peak counts reached two-thirds of the dynamic range of the 1420 Reticon's 14-bit A/D converter. A total of ten scans were accumulated to obtain an excellent spectrum with S/N ratio reaching $1x10^4$.

All-*trans* retinal purchased from Sigma was dissolved in n-hexane without further purification. High pressure liguid chromatography indicated that the all-*tran* retinal was greater than 95% pure(6). The dyes were all synthesized by the aldol condensation or Pd-catalyzed coupling procedures as described by Hassner *et al.*(7). The spreading solutions were prepared by adding a specific amount of dye molecules into Fisher spectrophotometry grade chloroform according to the published extinction coefficients(8).

3. Results and Discussion

a) Optical Properties of LB Monolayers

(i) Retinal

The normal incident UV/VIS absorption spectra of three retinal Langmuir-Blodgett monolayers are shown in Fig. 2, where the curve *a* and *b* are for the films which are transferred to glass substrates at surface pressure 10 and 12 dynes/cm respectively. The curve *c* is for the film which is deposited at surface pressure 16 dynes/cm where the LB monolayer on water subphase collapses. Compare the absorbances at the peak positions of the curves *a*, *b* and *c*. This comparison indicates that the surface densities of adsorbates increase with the surface pressures at which they are transferred. The peak positions of curves *a* and *b* in Figure 2 are at 385nm, close to the absorption maximum of retinal in methanol. However the absorption maximum of the collapsed film (curve *c*) is 10nm blue shifted from the curves *a* and *b*. This blue shift is probably generated by the molecules which are not in direct contact with the native hydrophilic glass surface, where high density of hydroxyl groups ($\simeq$ 4.6 OH groups/nm^2) have been found(9). It has long been known that solvent-induced shifts in $\pi \rightarrow \pi^*$ excitations energies are principally caused by dipole-mediated interactions that change the difference between the solute ground-state and excited-state dipole moments. With the perturbation theory and the classical reaction field methods, the shift in excitation energy $\hbar\Delta\omega_{eg}$ in the dipole approximation is given by(10):

$$\hbar\,\Delta\omega_{eg} = A\Delta\mu_{eg}(\mu_e + \mu_g) + B\Delta\mu_{eg}\,\mu_g \qquad 1$$

where $A = \frac{1}{a^3}\frac{n^2-1}{2n^2+1}$ and $B = \frac{2}{a^3}[\frac{\epsilon-1}{2\epsilon+1} \cdot \frac{n^2-1}{2n^2+1}]$ with n the index of refraction of the solution; ϵ the dielectric constant of the solution; a the effective cavity radius of the molecular site; μ_e and μ_g the solute dipole moments for the excited and ground states respectively. The first and second terms, respectively, are the reaction field experienced by the permanent dipole moment of the solute due to interaction with (1) the induced dipole moments of the surrounding molecules, and (2) the permanent dipole moments of the solvent and of other solute molecules. For a nonpolar solvent like n-hexane, the first term in Eq. 1 is much larger than the second term. Retinal solutions exhibit a general tendency that the increase in the polarity of solvent induces more red shift in $\pi \rightarrow \pi^*$ excitation energies of retinal (369nm in n-hexane, 380nm in methanol). The red-shift observed for retinal in solvent of increasing polarity indicates the dipole moment of this molecule increases in magnitude upon excitation. The conclusion of the increment of the dipole moment upon excitation is also reached by R. Mathies *et al.*(11) and Davidsson *et al.*(12) with an electrochromic technique.

The absorption band of the retinal LB film also exhibits broader breath than the solution phase. The full widths at half maximum (FWHM) of the absorption bands of retinal are 105nm (λ_{max}=385nm) in LB films, 85nm (λ_{max}=380nm) in methanol and 72nm (λ_{max}=369nm) in n-hexane. The solvent-induced broadening mechanism at finite temperature, as demonstrated from n-hexane to methanol, is the random modulation of electronic energy levels by fluctuations in the solvent degrees of freedom about their equilibrium positions(13). Similar modulation of

electronic energy levels can be induced in retinal LB films by fluctuations in hydroxyl groups on the glass substrates. The increased breadth of the LB film absorption can be accounted for as a result of additional effect due to substitutional disorder(14) and orientational disorder of the adsorbates.

(ii) Styryl Pyridinium Dyes

The absorption spectra of di-4-ASPPS and di-4-ANEPPS dye molecules were also measured and are shown in Figure 3(a) and (b) respectively. Compared to the peak positions of the dye molecules in methanolic solutions (see the solid lines in Figure 3(a) and (b)), blue-shifts are observed (dashed lines) in the monolayers. In these two molecules an unusual trend is noticed in the solvent-induced shifts in the absorption maxima; specifically, nonpolar organic solvents lead to bathochromic shifts relative to water while lipid vesicles which are normally assumed to provide a nonpolar membrane environment, lead to a blue-shifted spectrum. Fluhler *et al.*(8) have pointed out that such absorption change could be reconciled by considering the displacement of charge from the hydrophilic pyridine end to the hydrophobic aniline end of the molecule. Thus upon excitation the alteration in absorption is primarily the result of stabilization of the ground state due to the inability of solvent molecules to reorganize around the charge on the time scale of the absorption process. Nonpolar solvents raise the energy of the ground state, therefore decrease the excitation energy. In a membrane, the chromophore orientation is such that the charge in the ground state is exposed to the aqueous interface while the excited state is destabilized by the localization of its charge in the

hydrocarbon region; thus the energy of excitation increases relative to water and a blue shift is observed. A similar situation is found in the dye LB film. When it is transferred onto a native glass substrate, the charged hydrophilic pyridine comes into contact with the glass surface. The ground state is stabilized by the hydrogen bonding with the hydroxyl groups on the glass(15). However upon excitation, the excess charge accumulates near the aniline and this charge build up will be surrounded in a LB film by species with the same charge distribution rather than solvent molecules and thus a blue shift from the peak position of the methanolic solution is expected.

(b) **Surface-enhanced Raman Spectra**

(1) **All-trans Retinal**

Resonance Raman spectroscopy is one of the major techniques that can be used to study the chromophore structure of retinal. Assignments of the Raman (and IR) bands of the retinal isomers have been of fundamental importance as basis for the understanding of the experimental data on visual pigments and bacteriorhodopsin(16). In this regard, all-valence-electron quantum chemical calculations such as QCFF-π program(17) and MNDO procedure(18) are very useful for the generation of the stable molecular structures and force-field parameters which are used as the starting point of normal mode calculation. Reliable assignments require extensive vibrational measurements of model compounds with systematic isotope substitutions and refinement in the normal mode calculation.

Early assignments of the pre-resonance Raman (PRR) spectrum of all-trans-retinal were made by Rimai *et al.*(19). They classified the

observed Raman lines as either "lattice modes" of the vinyl carbon skeleton or "group modes" associated with C=O, CH_3 or vinyl hydrogen motions by arguing that vibrations of the β-ionone ring, because of their weak coupling with the conjugated π system, are unlikely to be observed in the PRR spectrum. Cookingham *et al.*(20) confirmed and extended these assignments with PRR spectra of desmethyl, butyl-substituted and β-ionone ring-modified retinal, as well as IR spectra of the unmodified retinals. More recently, Curry *et al.*(21) reported the Raman spectra of various deuterated *all-trans* retinals and assigned their Raman bands using the results of the normal mode calculation. The assignments of the Raman bands of retinal isomers were also reported by Mathies *et al.*(22) and Saito *et al.*(23). Our analysis of the SERS of retinal will be based on the Raman bands assignments proposed by Curry *et al.*(21).

In-Plane Vibrations The in-plane vibrations of the retinal chain can be classified into groups which are relatively isolated in frequency. The five C=C stretches and the C=O stretch appear between 1500cm^{-1} and 1700cm^{-1}. The fingerprint region from 1100 to 1400 cm^{-1} contains C-C stretches and CC-H in plane bends mixed in combinations which are strongly dependent on chain configuration.

(i) Double-Bond Streches

Only one peak is visible above 1620cm^{-1} in Figure 4. The Raman band at 1650 cm^{-1} in methanol is assigned to the C=O stretching of retinal. It is interesting to note that no band is found in the same region of the SERS of retinal. Also in the SERS of retinal, the major

peak at 1573cm^{-1} is shifted to 1582cm^{-1} with a shoulder at 1533cm^{-1}. Based on the Curry's assignments, this indicates that the bond order between C_{11} and C_{12} is increased with a concomitant decrease in C_{13}=C_{14} as retinal is adsorbed onto the silver island film.

(ii) **Fingerprint C-C Stretches**

The SERS of retinal exhibits no significant deviation of the C-C stretches from that of the free retinal in solution.

(iii) **Fingerprint CCH Bends and Methyl Group Deformations**

The most significant variation of the SERS of retinal in contrast to retinal in solution is seen in this region. The C_{14}-H bending mode at 1337cm^{-1} disappears in SERS spectrum and a weak new feature appears at 1364cm^{-1}. The 1364cm^{-1} band is visible only in the IR spectrum of retinal solution where it is assigned to the C_{15}-H bend based on a 15-D substitution shifts.

(iv) **Methyl Group Vibrations**

The 1397cm^{-1} in the SERS of retinal is slightly shifted from the observed 1402cm^{-1} frequency for the retinal in methanolic solution and is more intense than the adjacent 1445cm^{-1} CH_3 deformation band which is masked by the solvent mode in the PRR spectrum of the methanolic solution of retinal.

Out-of-Plane Vibrations In the retinal SERS has two bands which appear at 975cm^{-1} and 956cm^{-1} respectively. They are clearly resolved, however these two bands merge into a single peak at 968cm^{-1} in the PRR

spectrum of retinal methanolic solution. For a A-term enhanced planar molecule, this A_u-type vibration is Franck-Condon inactive. The moderate intensity of the 968cm^{-1} mode indicates that the local plane of the ethylene is perturbed upon excitation.

Discussions The comparison between the SERS of retinal adsorbed on a silver island film and the PRR spectrum of retinal free in methanol solution indicates that most of the variations are confined to the neighborhood of the carbonyl group of retinal. This is consistent with the expectation that the C=O group of the retinal comes in direct contact with the silver film. The perturbed normal modes are the C_{14}-H, C_{15}-H bends, C_{14}-C_{15}, C_{13}=C_{14} and C_{15}=O stretches. Besides these alterations, the C_{10}-C_{11} and C_8-C_9 stretching bands also show an interesting intensity variation as the excitation wavelength is changed. In Figure 5 is the SERS spectra of retinal at the excitation of different argon ion laser lines. In this Figure, the averaged power of the incident laser light is fixed at 5mW for each wavelength. The Raman enhancement profile of the normal modes which involve the polyene in-plane chain vibrations can be well accounted for by the A-term enhancement of the $\pi\pi^*$ electronic excitation(24). From the observation of the perturbed C_{14}-H and C_{15}-H bending modes in the SERS spectrum, the carbonyl group of retinal is anchored to the surfaces of silver particles with a specific tilt angle. This intensity variation of C_{10}-C_{11} and C_8-C_9 stretches with respect to the excitation wavelength could then be explained by different wavelength dependent contributions of the tangential and normal fields of the island films.

The surface-enhanced Raman scattering cross-section can be estimated by comparing the SERS intensity of adsorbed molecules with the Raman scattering intensity of the same molecules which are free in solution(25):

$$\sigma_{sers} = \frac{I_{gf}^{sers}}{I_{gf}^{R}} \frac{I_o^R(\nu_o)}{I_o^{sers}(\nu_o)} \frac{N_r}{N_{sers}} \frac{F_r S_r(\nu_r) E_r(\nu_r)}{F_{sers} S_{sers}(\nu_s) E_{sers}(\nu_s)} \sigma_R \qquad 2$$

where I_{gf}^{sers}, I_{gf}^{R} are the measured Raman intensities of adsorbed and free molecules for a specific Raman transition g → f. I_0^R and I_0^{sers} are the averaged laser intensities used for the PRR and SERS measurements. N is the number of molecules which are contained in the scattering volume. $F(\theta)$ is the fraction of the scattered light which is imaged into the spectrometer. $S(\nu)$ is the transmittance of the Raman scattered light out of the sample; it is equal to 1 for the measurement of SERS and for PRR spectrum it is estimated from the absorption spectrum of the retinal methanolic solution. $E(\nu_r)$ is the combined throughput efficiency of the spectrometer and detector for the Raman scattered frequency ν_r; and $\sigma(\nu_0)$ is the Raman scattering cross-section for an excitation frequency ν_0. The number of the excited free retinal molecules is estimated from the absorbances of retinal methanolic solution using the known extinction coefficient ε_{380}=42884 $M^{-1}cm^{-1}$(26). The ω^4 dependence and the combined efficiency of the spectrometer and the detector can be removed with this normalization scheme. The major uncertainties are therefore the estimated errors of the number of the excited molecules, the collection efficiency and the averaged laser

power. The errors in the measurement of the Raman enhancement, which are listed in Table I are estimated to be less than 30%. The Raman enhancement calculated from the surface plasmon excitation model(27) is plotted in Figure 6, where the solid line is the averaged enhancement factor for 1580cm^{-1} Raman line while this factor on the equator of silver oblate spheroids is indicated by the dashed line. This enhancement has been averaged over the distribution function of the silver particle size which is extracted from the measured absorption spectrum of a 55Å thick silver island film. The maximum calculated value is roughly a factor of 3 smaller than that which is measured (see circles in Figure 6). A part of this deviation may be explained by the irregular particle shape of the actual unannealed silver island film. An additional enhancement due to the lightning rod effect which is caused by the sharp boundary of the irregular particle is expected. However other enhancement mechanisms cannot be excluded by this experiment. The calculated absorption spectrum of a 55Å thick silver island film is also included for comparison as the top graph in Figure 6. The position of the enhancement peak (circles in Figure 6) is not overlapped with the absorption maximum of the silver island film. The reason is attributed to the change of the dielectric function outside the silver particles by the deposited retinal LB film.

(2) di-4-ASPPS and di-4-ANEPPS dyes

Most of the C=C double bonds in the di-4-ASPPS molecule are arranged in two phenyl rings with one ethylene unit as the connection bridge between two rings in a trans configuration. The di-4-ASPPS is therefore expected to have a similar vibrational structure as trans-

stilbene or 4-styrylpyridine. The detailed assignments of trans-stilbene Raman (or IR) bands were proposed by Meić *et al.*(28) by comparing the vibrational spectra of nine partially deuterated trans-stilbene molecules. Theoretical investigation of the ground and excited states vibrational structures of trans-stilbene using QCFF-π method was reported by Warshel *et al.*(29). We have also performed MNDO calculation on a simplified di-4-ASPPS molecule by attaching methyl groups to the nitrogen atoms of the pyridine and aniline. Although the calculated vibrational frequencies with the MNDO method are generally 10% higher than the observed values(30), the result exhibits five types of vibrational frequencies. This agrees with the Warshel's calculation of trans-stilbene.

In-Plane Vibrations The MNDO calculation shows a large vibrational gap between 1700 and 3000cm^{-1}. Above 3000cm^{-1} the vibrational peaks are generally assigned to the C-H stretches. These normal modes will not be discussed because of their low intensities in Raman spectrum.

(i) Ring Stretches and Ethylene C=C stretch

The SERS of di-4-ASPPS and di-4-ANEPPS are shown in Figure 7(a) and (b) respectively. Above 1600cm^{-1}, two modes at 1641cm^{-1} and 1620cm^{-1} are observed for both di-4-ASPPS and di-4-ANEPPS. The 1641cm^{-1} is assigned to the ethylene C=C stretch. The 1620cm^{-1} comprises of the same ethylene stretch with the combination of the pyridine ring stretch mode. Trans-stilbene exhibits a much more intense C=C stretch peak at 1644cm^{-1}. This peak is shifted to 1607cm^{-1} as the hydrogens of the ethylene are deuterated. The 1585cm^{-1} of di-4-ASPPS is the in-plane

ring stretch. This band is shifted to 1602cm^{-1} in di-4-ANEPPS. The shoulder band at 1551cm^{-1} in Figure 7(a) is also sensitive to the substitution of aniline ring of di-4-ASPPS by a naphthalene and is up-shifted to 1566cm^{-1} in di-4-ANEPPS. It is assigned to the aniline C-N stretch according to the MNDO analysis. The three bands at 1438, 1472 and 1518cm^{-1} in di-4-ASPPS are due to the benzene and pyridine ring stretches. The first two peaks are shifted to 1428 and 1478cm^{-1} in di-4-ANEPPS and are attributed to the benzene (naphthalene) ring stretches.

(ii) C-C Stretches and C-H in-plane Bending

As in retinal, the vibrational bands between 1100cm^{-1} and 1400cm^{-1} are assigned to the C-C stretches and CC-H in-plane bending. The most distinguishable feature in this region is the double-peak feature at 1173 and 1211cm^{-1} in Figure 8. The 1173cm^{-1} is assigned to the in phase ring-C_e stretch. This band appears at 1199cm^{-1} in trans-stilbene. The 1211cm^{-1} is due to the pyridine mode because the same peak appears in 4-styrylpyridine but it vanishes in trans-stilbene. In Figure 7(a), two vibrational bands at 1316cm^{-1} and 1331cm^{-1} are attributed to the C-H in-plane bend which becomes an unresolved peak at 1328cm^{-1} in Figure 8(b).

(iii) In-Plane Ring Deformations

From the MNDO calculation, six in-plane ring deformations occur between 500 and 900cm^{-1} with four associated with the benzene ring and two with the pyridine ring. The low frequency part of the SERS of di-4-ASPPS and di-4-ANEPPS is shown in Figure 8. Two peaks which appear at

887cm^{-1} and 740cm^{-1} in di-4-ASPPS (solid line) vanish in the di-4-ANEPPS spectrum (solid circles). The quality and resolution of the spectra, however do not allow further assignments and comparisions.

Out-of-Plane Vibrations The vibrational modes below 500cm^{-1} are generally assigned to the molecular skeleton out-of-plane deformations according to the MNDO calculation. Several bands are observed in this region for di-4-ASPPS but no assignments are made. One of the out-of-plane vibrations, which has a significant higher frequency is the A_u-type out-of-plane wag of the ethylene hydrogens which occurs at 967cm^{-1}. The moderate intensity of this band in the spectra of di-4-ASPPS and di-4-ANEPPS indicates that these two molecules are not strictly planar.

Discussion The Raman enhancement factor of di-4-ANEPPS at the excitation of 4579Å laser line is estimated to be 5.8×10^3 using Eq.2. This value is significantly lower than that of retinal. The result agrees with the model proposed by Weitz *et al.*(31), where a hierarchy of the Raman enhancement factor is found with typical values of 10^5 for normal Raman scattering, 10^3 for resonant Raman scattering and 10^{-1} to 10 for fluorescence. The difference in the enhancement is understandable as the surface plasmons of metal particles are regarded as the major scatterers. The Raman scattering intensity from the surface is therefore relatively constant no matter whether the adsorbed molecules are resonant or not. However as the enhancements are calculated from the ratio of the scattering intensity on the surface and in bulk, it will be very much smaller for a dye molecule which is known to exhibit

strong scattering in bulk.

The resonance enhanced Raman spectrum of di-4-ANEPPS monolayer on a glass substrate was also observable. The SERS and unenhanced Raman spectra of a monolayer of di-4-ANEPPS at the excitations of 4579Å and 4965Å laser lines show no observable deviations (see Figure 9(a) and (b)) for the 1602cm^{-1} and 1173cm^{-1} Raman lines. This indicates that the observed Raman enhancement of the dye molecules on silver island film are effected by the classical field enhancement mechanism by way of resonant excitation of surface plasmons.

4. Conclusion

An excellent Raman spectrum of a monolayer can be obtained with the enhancement of a silver-island film under excitation with a relatively low laser power. The combination of SERS and optical multichannel detection techniques appear useful for the investigations of the vibronic structures of molecules which are easily isomerized or photodegraded by the laser light. *All-trans*-retinal and two kinds of pyridinium styryl dye molecules have been used in this study. These molecules are deposited onto silver-island films by using the Langmuir-Blodgett techniques to obtain monolayers with good optical quality and accurately controlled surface density. The SERS and optical absorption spectroscopies are used to characterize the monolayer-coated silver-island films. A Raman enhancement factor of $3x10^6$ for retinal and $6x10^3$ for the styryl pyridinium dye molecules is obtained.

Acknowledgement

This research was supported by a contract from the U.S. Army contract #DAMD17-85C-8136 and L. M. Loew is pleased to acknowledge support from the U. S. Public Health through NIH Grant GM 35063. For the interpretation of Fig. 5, we thank the referee.

Table I The measured Raman enhancement factors of the C=C stretching band for *all-trans*-Retinal on a 55Å thick silver-island film.

Excitation Wavelength	Self-Absorption Factor $S_r(1573cm^{-1})$	$\frac{I_{gf}^{sers}}{I_{gf}^{R}} \frac{I_0^R}{I_0^{sers}}$	Molecular Resonance	Raman Enhancement
5145Å	0.984	78.0	0.648	$(3.0\pm1.0)\times10^5$
5017Å	0.977	77.1	0.887	2.9×10^5
4965Å	0.974	66.5	1.008	2.5×10^5
4880Å	0.970	48.3	1.307	1.8×10^5
4765Å	0.928	31.5	2.046	1.1×10^5
4579Å	0.710	13.0	4.951	3.7×10^4

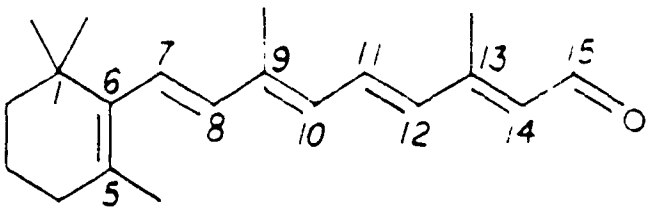

A

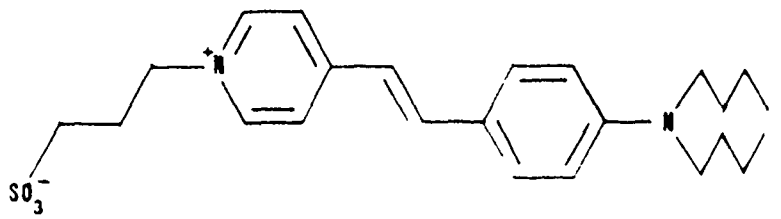

B

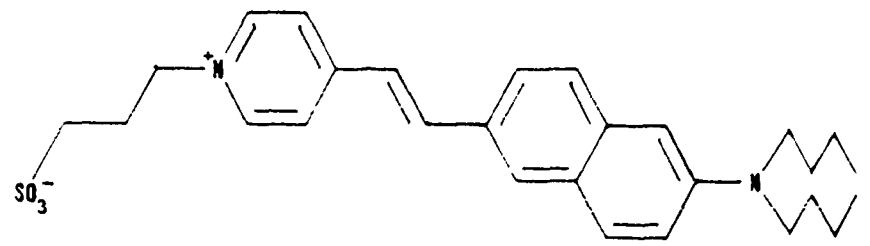

C

Fig. 1. The chemical structures of (a) all-trans retinal, (b) di-4-ASPPS and (c) di-4-ANEPPS molecules.

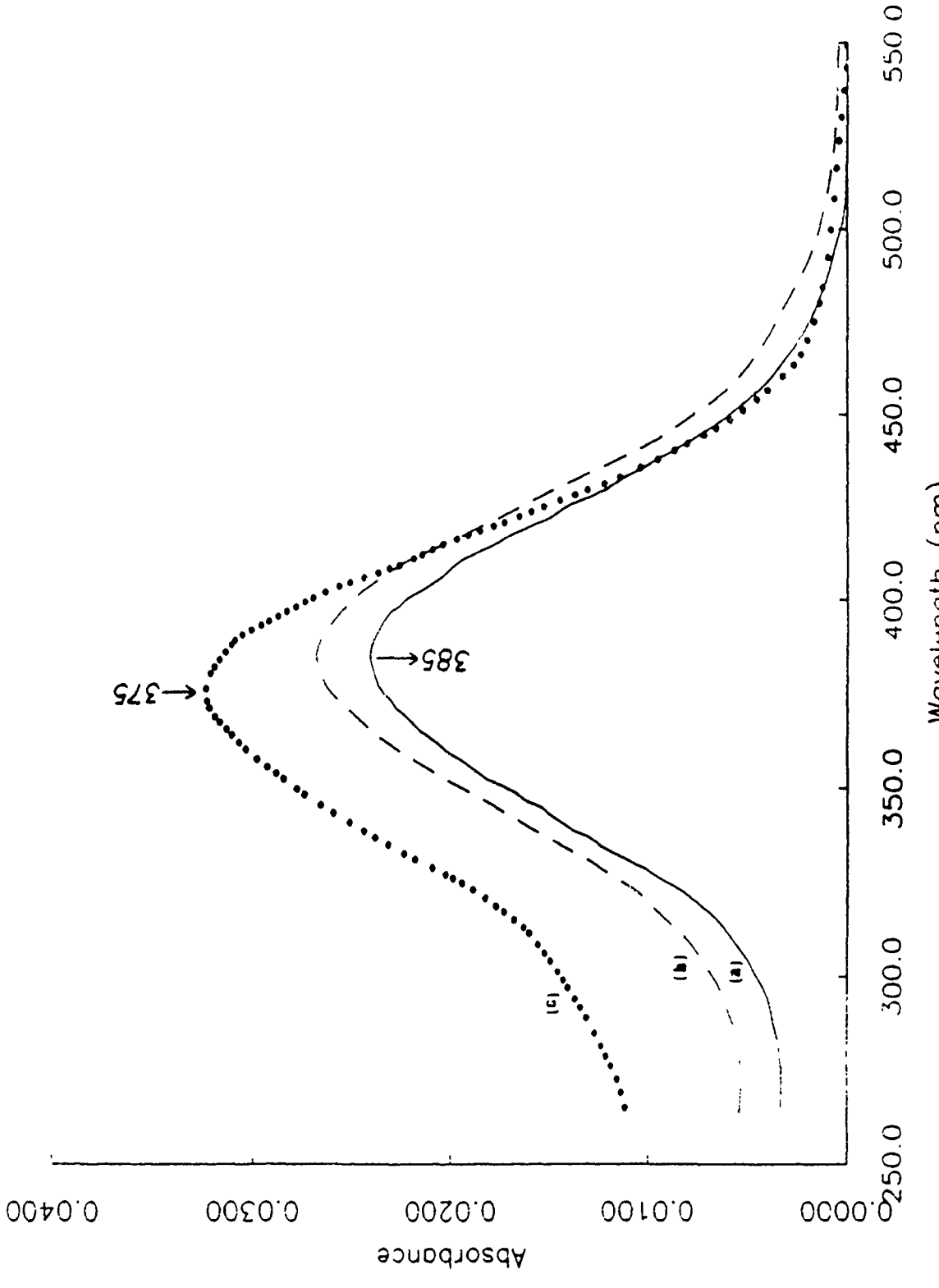

Fig. 2. The absorption spectra of all-trans retinal Langmuir-Blodgett films which are deposited on glass substrates at surface pressure of (a) 10, (b) 12 and (c) 16 dynes/cm respectively.

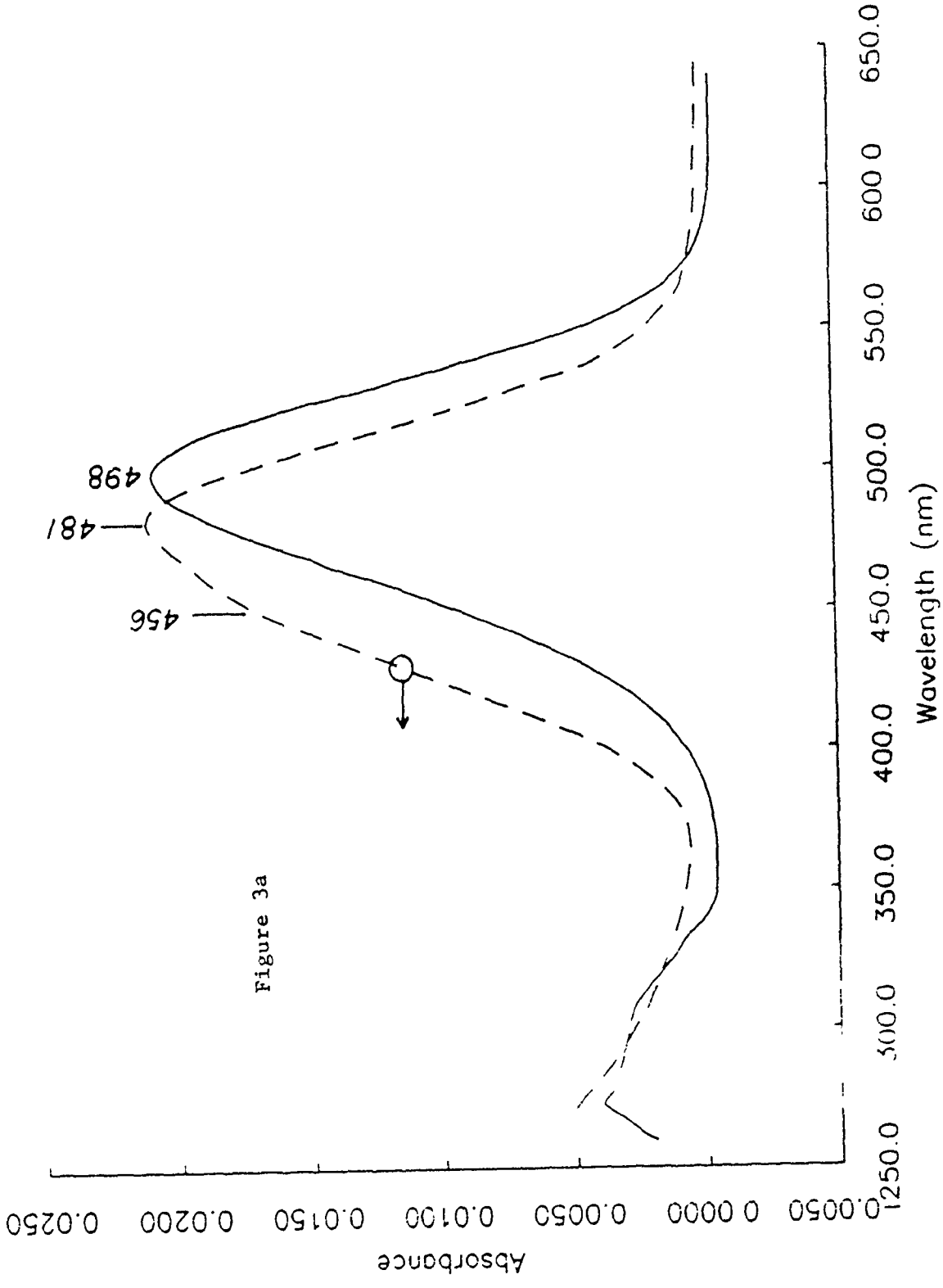
Absorbance
0.0250
0.0200
0.0150
0.0100
0.0050
0.0000
-0.0050
1250.0
300.0
350.0
400.0
450.0
500.0
550.0
600.0
650.0
Wavelength (nm)
498
481
456

Figure 3a

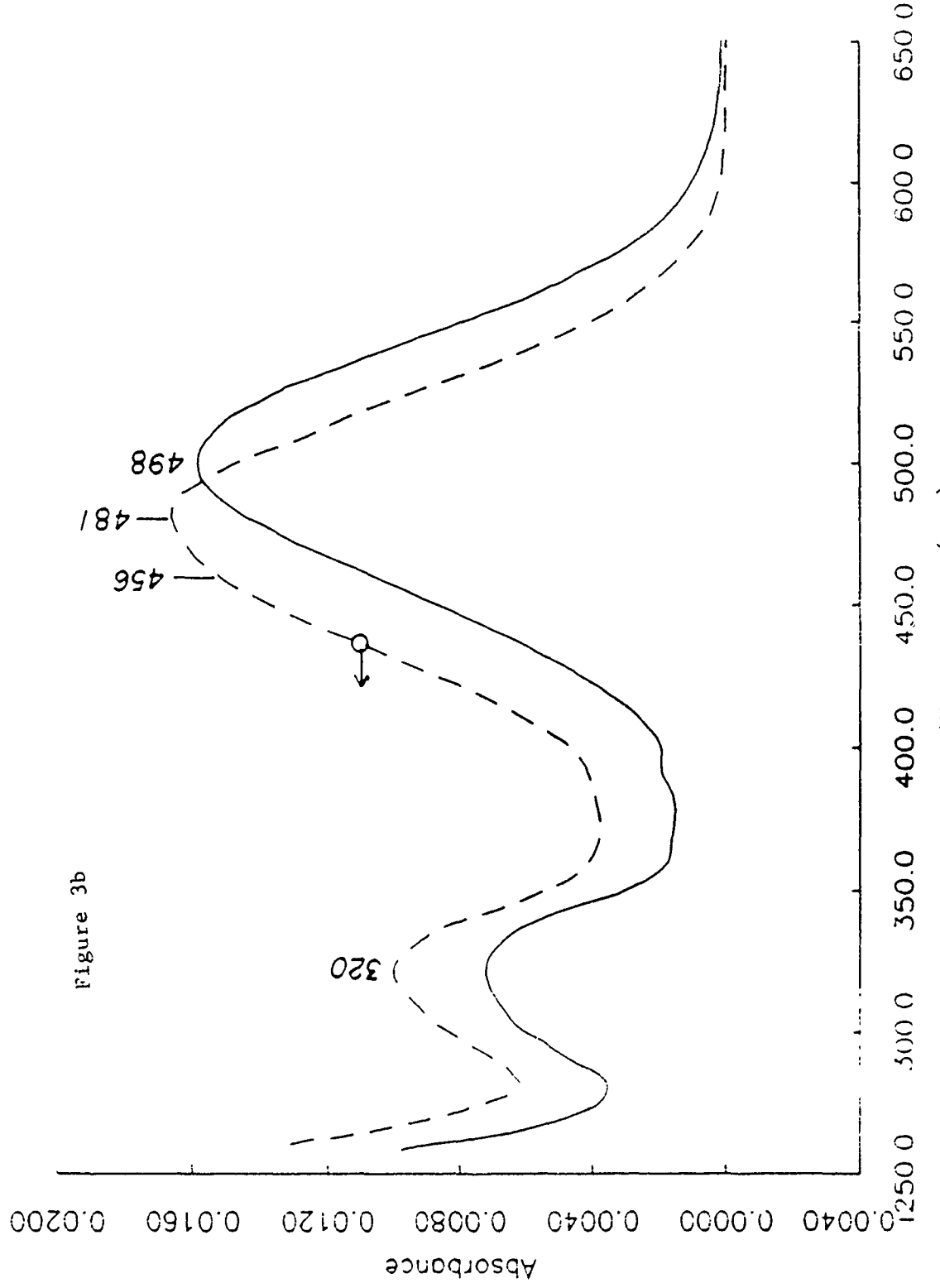

Fig. 3. The absorption spectra of (a) di-4-ASPPS and (b) di-4-ANEPPS LB films which are deposited onto glass substrates at surface pressure of 20 dynes/cm. The solid lines in (a) and (b) are for the absorption spectra of the dye molecules in methanolic solutions.

Normalized Raman Intensity
0.00
0.25
0.50
0.75
1.00
1.25
1.50
900.0
1000.0
1100.0
1200.0
1300.0
1400.0
1500.0
1600.0
1700.0
Raman Shift (cm-1)
1008
s
1164
1161
1196
1198
1271
1272
1302
1337
1364
1397
1445
s
1533
1573
1582
1650

Figure 4a

Figure 4b

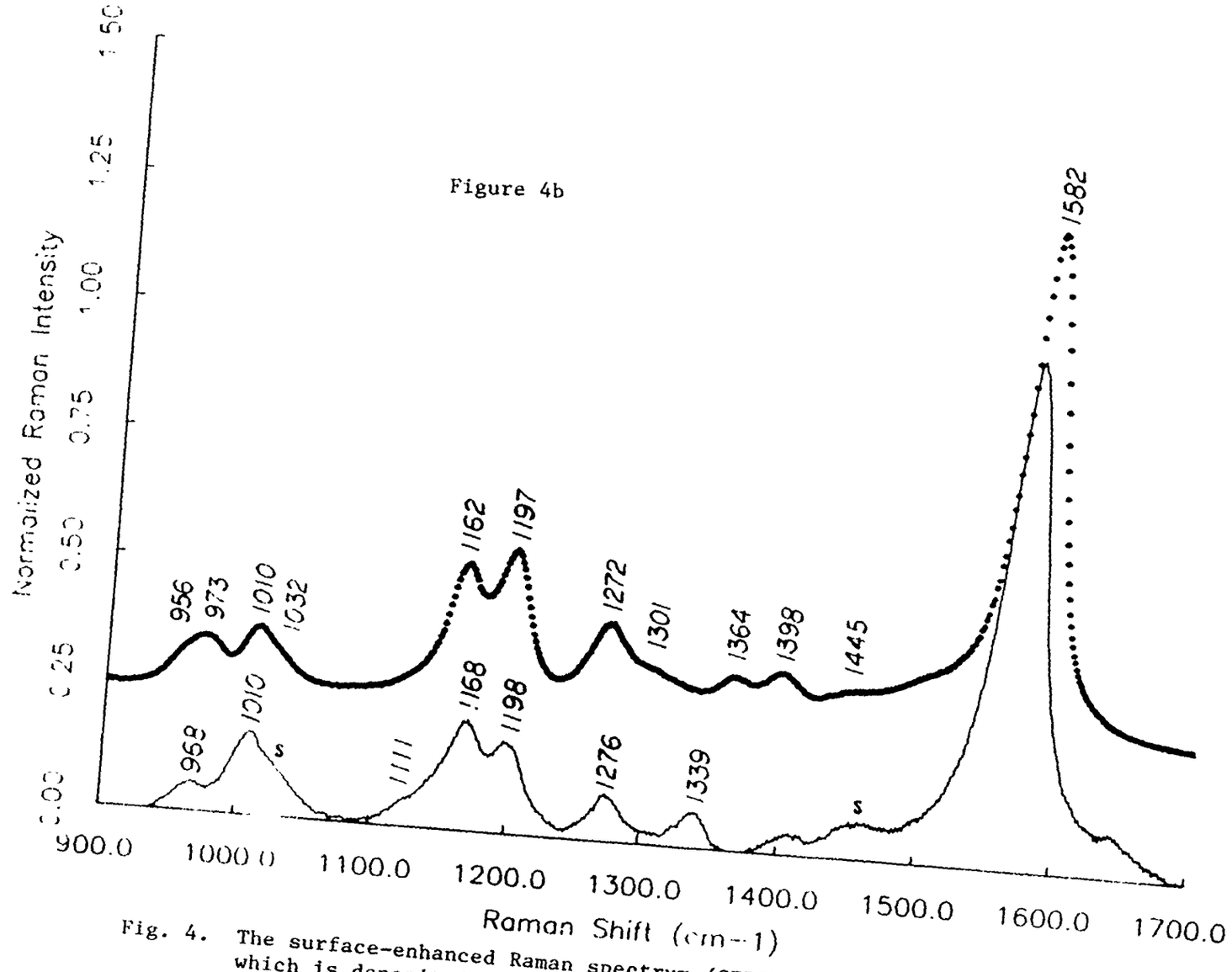

Fig. 4. The surface-enhanced Raman spectrum (SERS) of a retinal LB film which is deposited on a 55Å thick silver island film is shown in (a) for excitationof 5145Å and (b) 4579Å argon ion laser lines (solid circles). The Raman spectrum of retinal in methanol solution is also included for comparison (solid line). Note that the peaks marked by the letter "S" are due to the Raman bands of methanol.

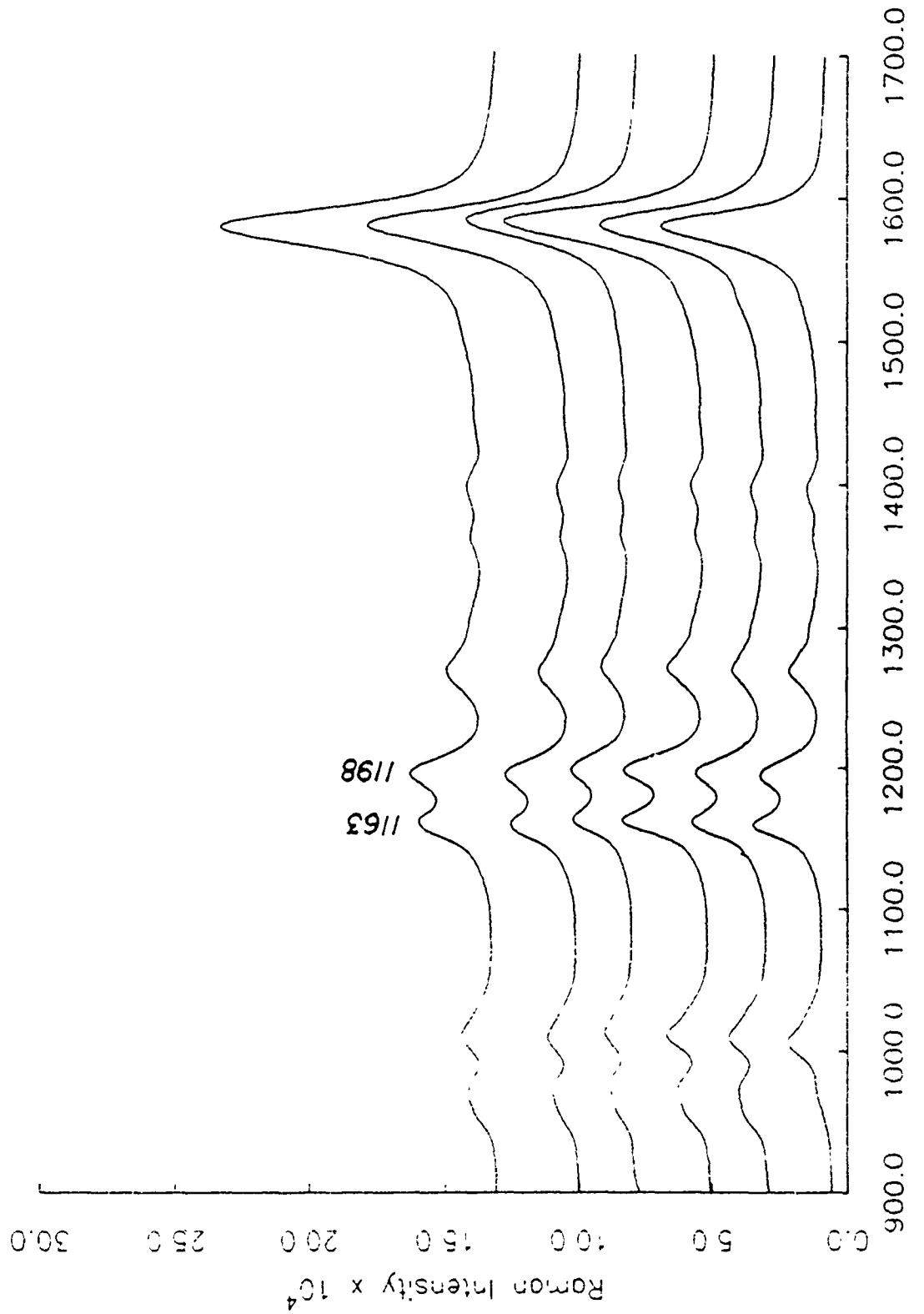

Fig. 5. The SERS of a retinal LB film at excitation of 5145Å, 5017Å, 4965Å, 4880Å, 4765Å and 4579Å argon ion laser lines are shown (from bottom to top). Note that the intensities of the 1163 cm^{-1} and 1198 cm^{-1} bands vary as the excitation wavelength is changed.

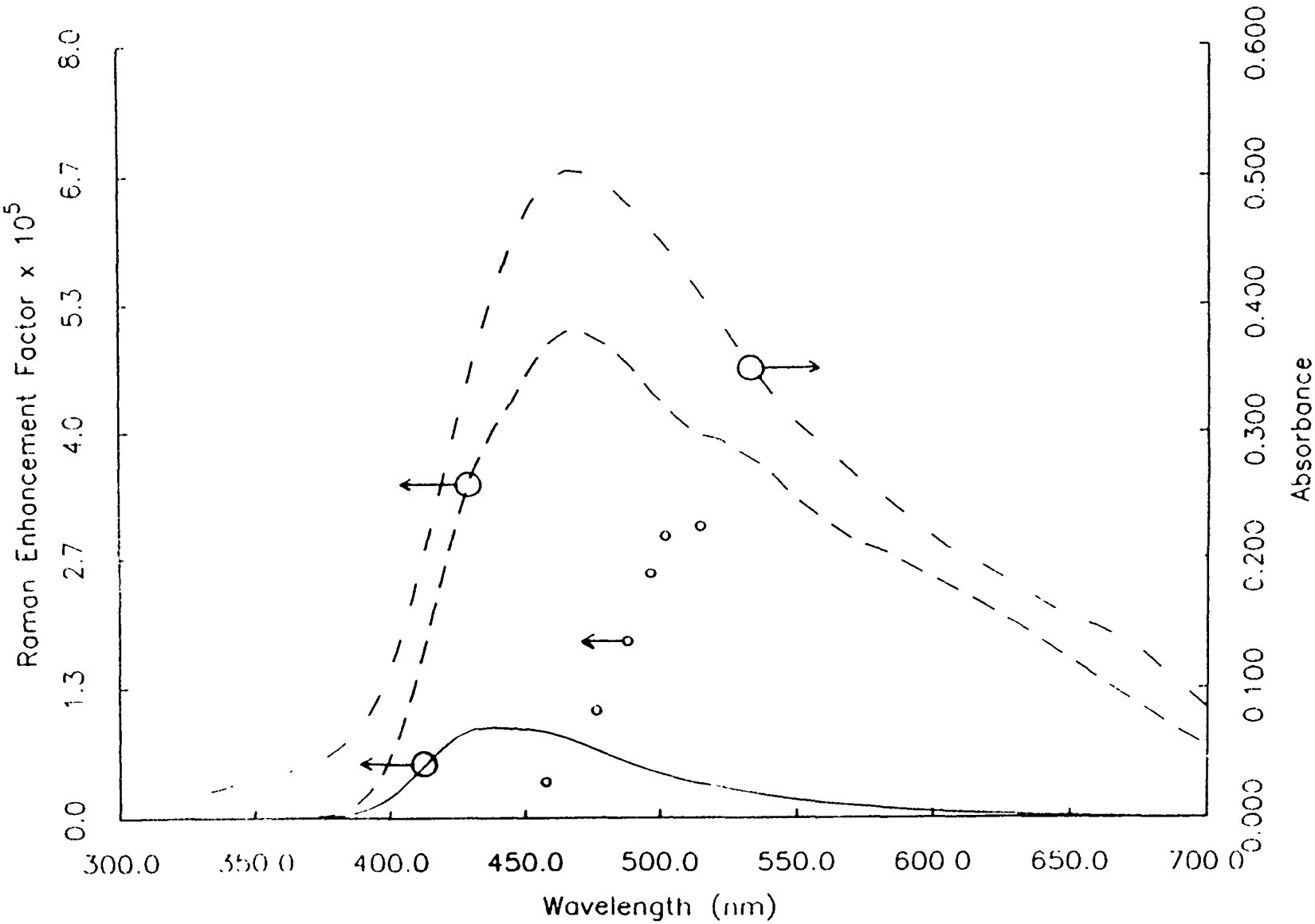

Fig. 6. The Raman enhancement factor of the retinal 1580 cm^{-1} band. The experimental data are shown in open circles, while the calculated curves for a set of silver particles with various alues of aspect ratio are indicated by the dashed line (on the equators of the silver oblate spheroids) and the solid line (averaged over the surfaces of the particles). The calculated absorption spectrum for a 55A thick silver island film (dashed-dot-dot line) is included for comparison.

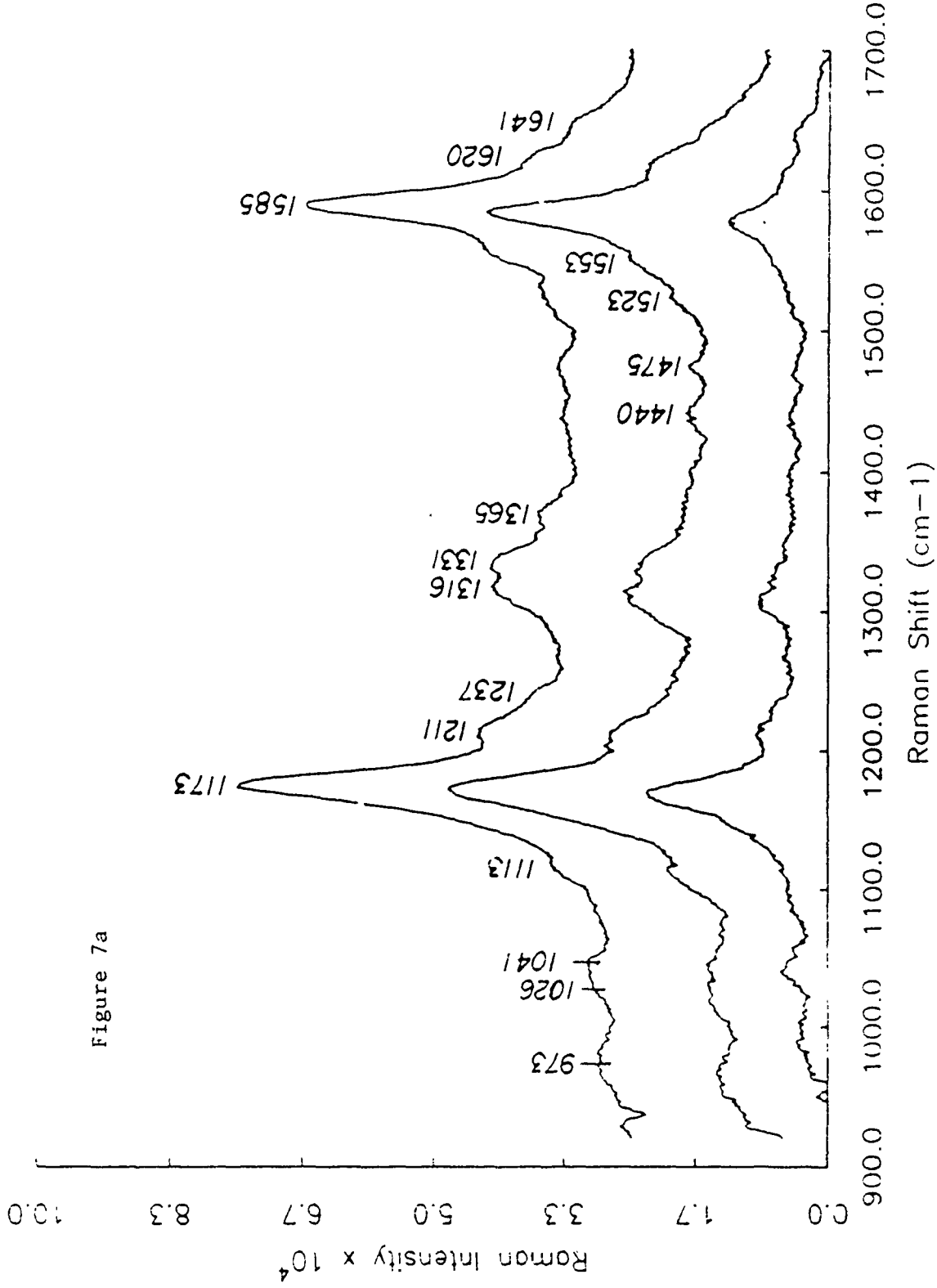
Raman Intensity x 10^4
0.0
1.7
3.3
5.0
6.7
8.3
10.0
900.0
1000.0
1100.0
1200.0
1300.0
1400.0
1500.0
1600.0
1700.0
Raman Shift (cm−1)
973
1026
1041
1113
1173
1211
1237
1316
1331
1365
1440
1475
1523
1553
1585
1620
1641

Figure 7a

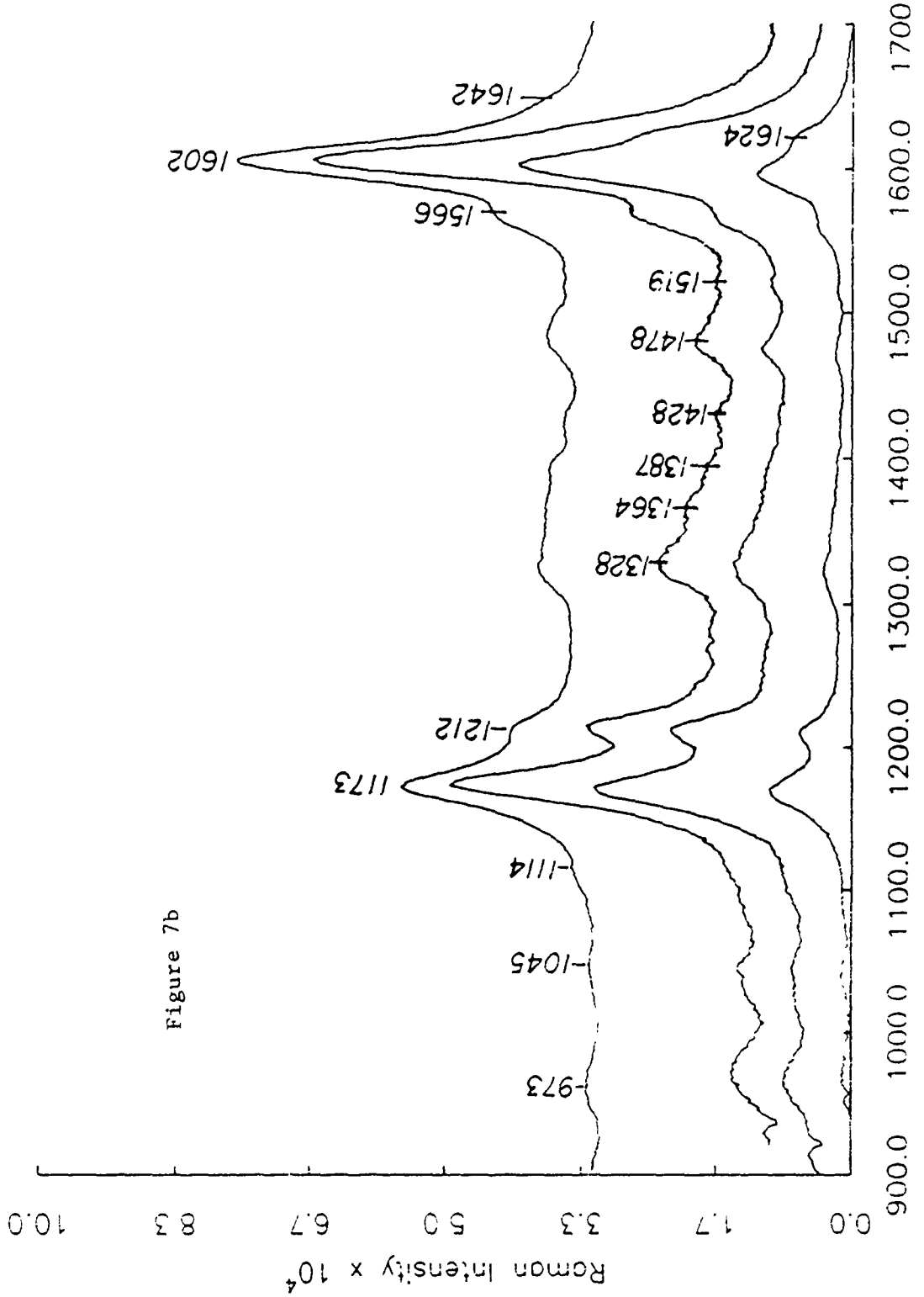

Fig. 7. The SERS of a (a) di-6-ASPPS and (b) di-4-ANEPPS dye LB film which is deposited on a 55Å thick silver island film. The excitation wavelengths are 5145Å, 4965Å and 4880Å (from bottom to top) for (a); and are 5145Å, 4965Å, 4880Å and 4579Å (from bottom to top) for (b).

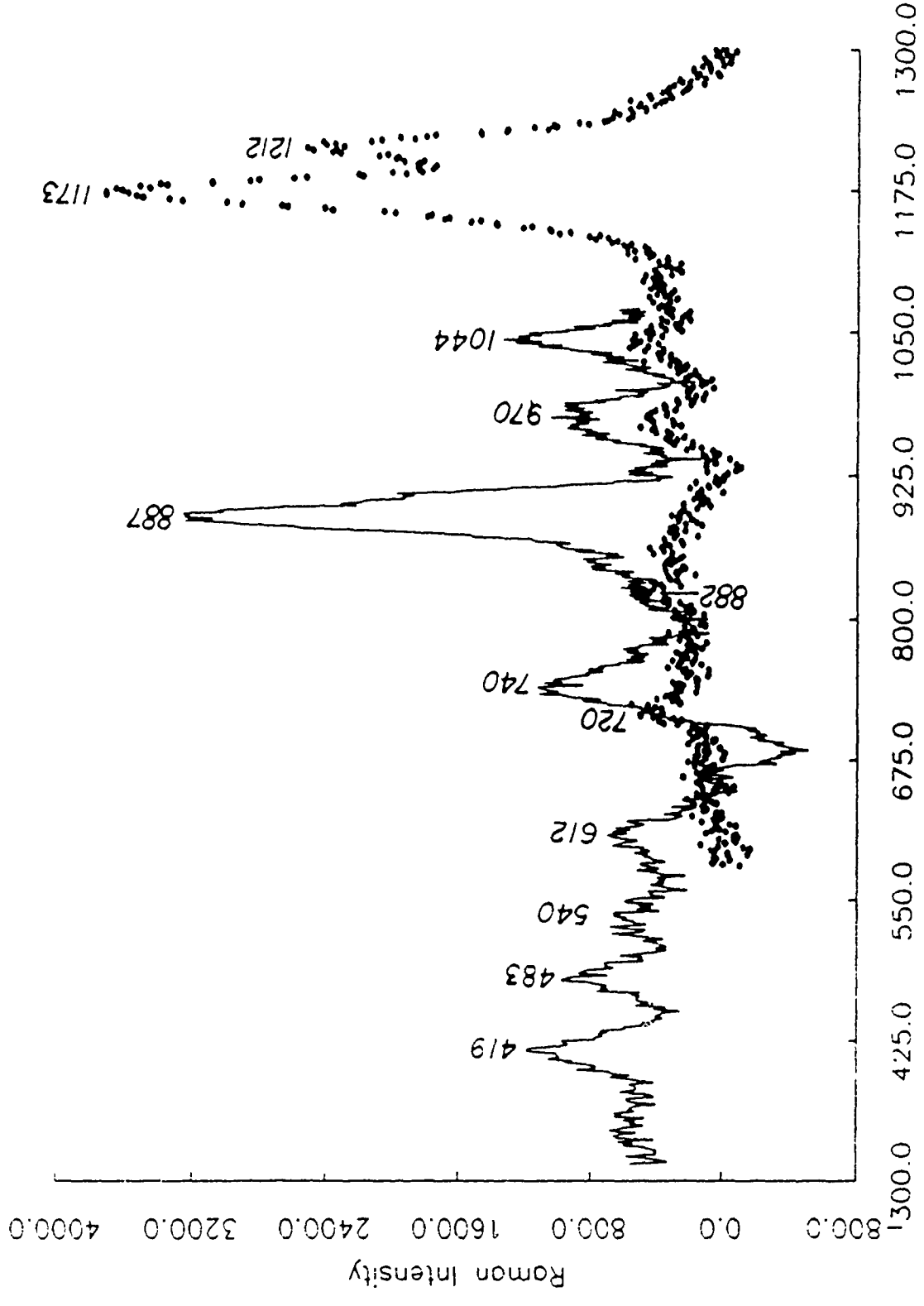

Fig. 8. The SERS of di-6-ASPPS (solid line) and di-4-ANEPPS (solid circles) LB films in low frequency region. The exciting light source is the 4579A line of an argon ion laser.

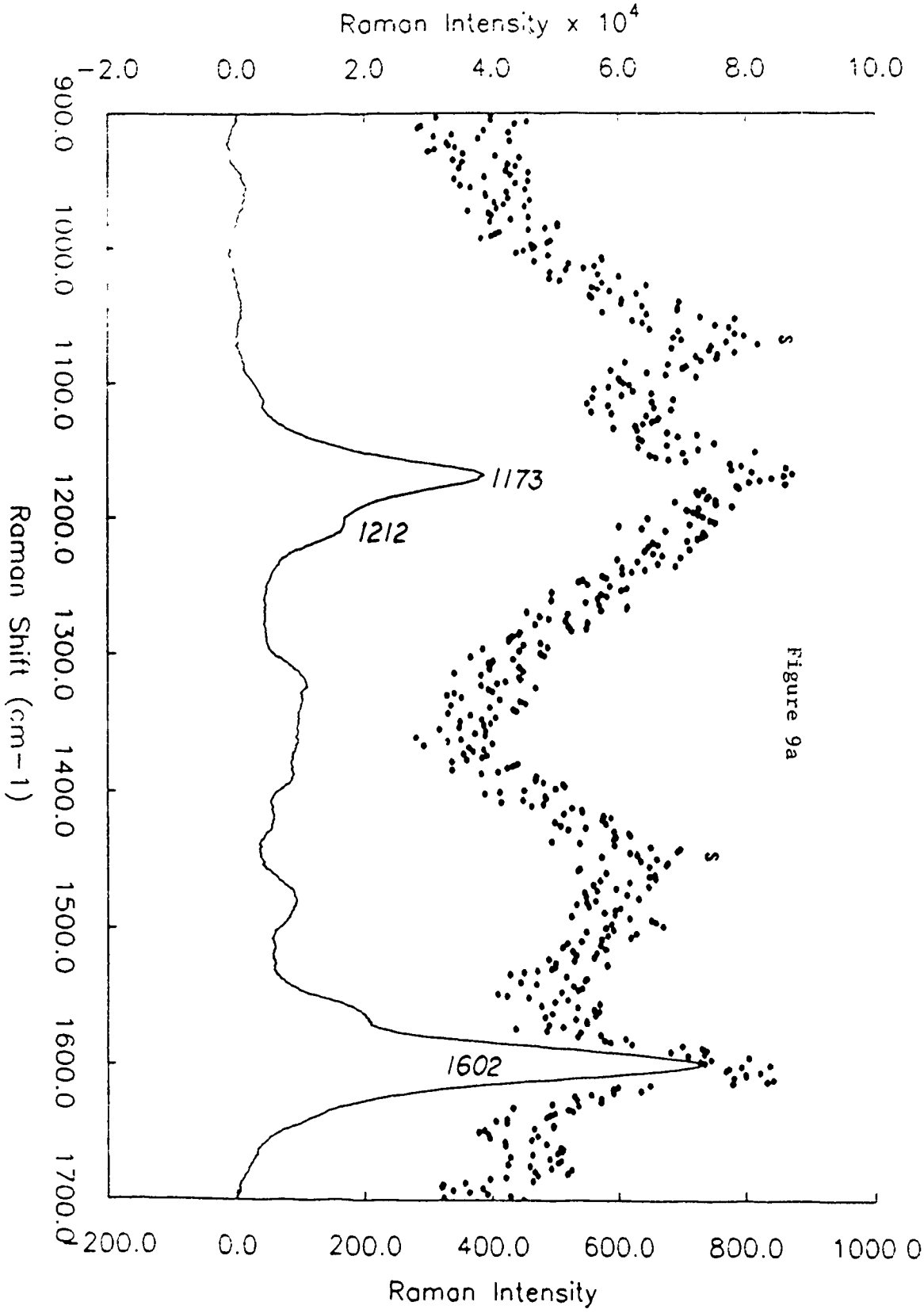
Raman Intensity x 10^4
−2.0
0.0
2.0
4.0
6.0
8.0
10.0
900.0
1000.0
1100.0
1200.0
1300.0
1400.0
1500.0
1600.0
1700.0
Raman Shift (cm−1)
1173
1212
1602
S
S
200.0
0.0
200.0
400.0
600.0
800.0
1000.0
Raman Intensity

Figure 9a

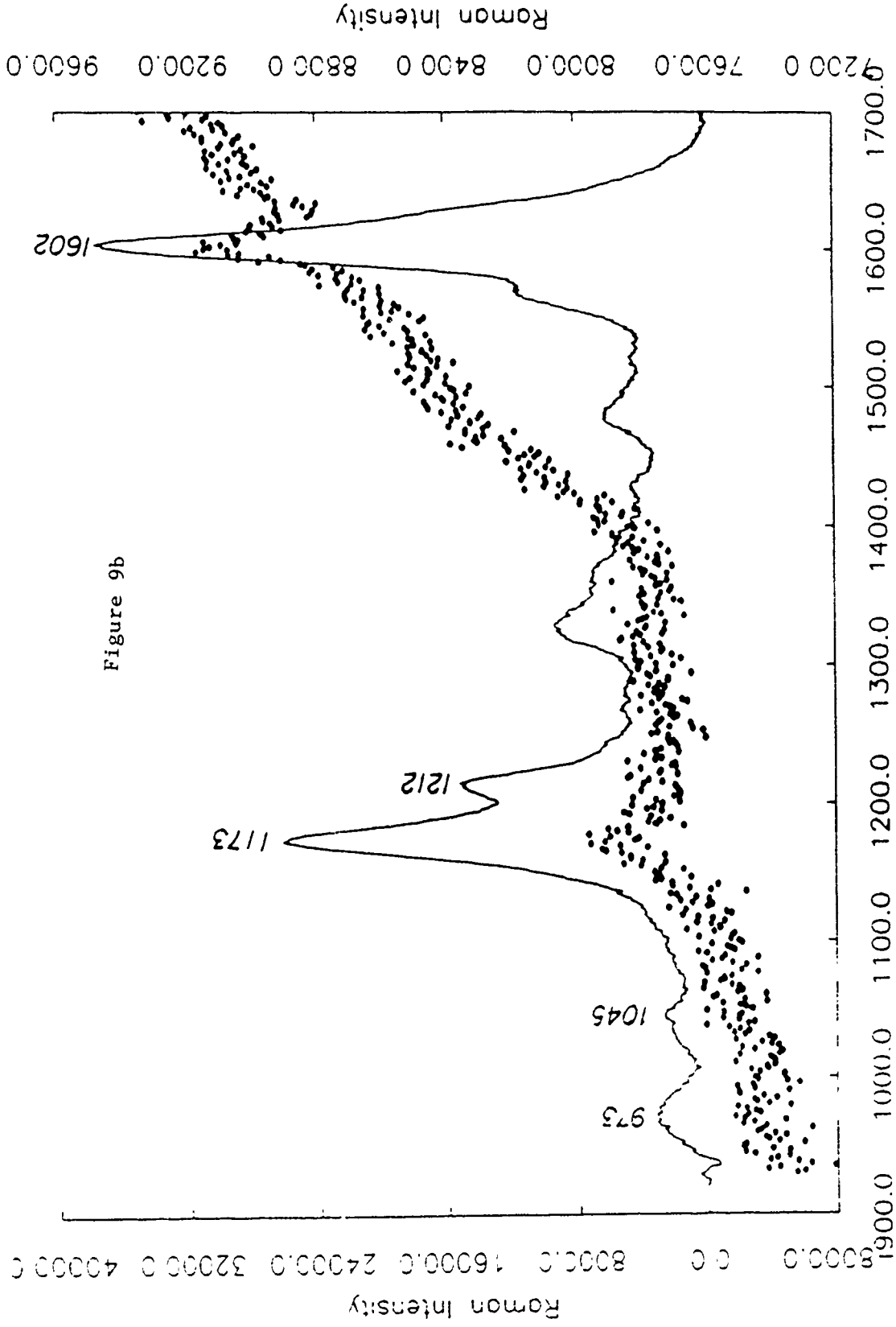

Figure 9b

Fig. 9. The unenhanced Raman spectrum of a di-4-ANEPPS LB film on a glass substrate (solid circles) and its SERS spectrum on a silver island film (solid line) are shown in (a) as excited by the 4579Å and (b) 4965Å lines of an argon ion laser. The bands marked by the letter "S" in (a) is due to the unevaporated methanol which is used as the spreading solvent.

References

1. R. R. Birge, *Annu. Rev. Biophys. Bioeng.* 10, 315 (1981).
2. D. Gross, L. M. Loew, and W. W. Webb, *Biophys. J.* 50, 339 (1986).
3. K. B. Blodgett, *J. Am. Chem. Soc.* 57, 1007 (1935).
4. P. Royer, J. P. Goudonnet, R. J. Warmack, and T. L. Ferrell, *Phys. Rev.* B35, 3753 (1987).
5. S. A. Asher, C. R. Johnson, and J. Murtaugh, *Rev. Sci. Instrum.* 54, 1657 (1983).
6. M. A. Marcus, A. T. Lemley, and A. Lewis, *J. of Raman Spectrosc.* 8, 22 (1979).
7. A. Hassner, D. Birnbaum, and L. M. Loew, *J. Org. Chem.* 49, 2546 (1984).
8. E. Fluhler, V. G. Burnham, and L. M. Loew, *Biochemistry* 24, 5749 (1985).
9. J. B. Peri and A. L. Hensley, Jr., *J. Phys. Chem.* 72, 2926 (1968).
10. C. C. Teng and A. F. Garito, *Phys. Rev.* B28, 6766 (1983).
11. R. Mathies and L. Stryer, *Proc. Natl. Acad. Sci. USA* 73, 2169 (1976).

    M. Ponder and R. Mathies, *J. Phys. Chem.* 87, 5090 (1983).
12. Å. Davidsson and L. B. Å. Johansson, *J. Phys. Chem.* 88, 1094 (1984).
13. A. B. Myers, M. O. Trulson, J. A. Pardoen, C. Heeremans, J. Lutenburg, and R. A. Mathies, *J. Chem. Phys.* 84, 633 (1986).
14. B. N. J. Persson, A. Liebsch, *Phys. Rev.* B28, 4247 (1983).
15. W. Pohle and P. Zink, *Z. Phys. Chem.* (Wiesbaden) 109, 205 (1978).

16. For review see, *Methods in Enzymology*, Vol.88, Part I, ed. L. Packer; Academic Press: New York, 1982.

17. A. Warshel, M. Karplus, *J. Am. Chem. Soc.* 96, 5677 (1974).

18. J. S. Dewar and W. Thiel, *J. Am. Chem. Soc.* 99, 4899 (1977).

19. L. Rimai, D. Gill, and J. L. Parson, *J. Am. Chem. Soc.* 93, 1353 (1971).

20. R. E. Cookingham, A. Lewis, and A. T. Lemley, *Biochemistry* 17, 4699 (1978).

21. B. Curry, A. Broek, J. Lutenburg and R. Mathies, *J. Am. Chem. Soc.* 104, 5274 (1982).

22. B. Curry, I. Palings, A. D. Broek, J. A. Pardoen, J. Lugtenburg, and R. Mathies, *Adv. Infrared Raman Spectrosc.* 14, 236 (1983).

23. S. Saito and M. Tasumi, *J. of Raman Spectrosc.* 14, 236 (1983).

24. R. Callender and B. Honig, *Ann. Rev. Biophys. Bioeng.* 6, 33(1977).

25. J. M. Dudik, C. R. Johnson, and S. A. Asher, *J. Chem. Phys.* 82, 1732 (1985).

26. R. S. Becker, K. Freedman, and C. Lenoble, *J. Phys. Chem.* 90, 4334 (1986).

27. A. Wokaun, *Molecular Physics* 56, 1 (1985).

28. Z. Meić and, H. Güsten, *Spectrochim. Acta* A34, 101 (1978).

29. A. Warshel, *J. Chem. Phys.* 62, 1 (1975).

30. M. J. S. Dewar, G. P. Ford, M. L. Mckee, H. S. Rzepa, W. Thiel, and Y. Yamaguchi, *J. of Molecular Structure* 43, 135 (1978).

31. D. A. Weitz, S. Garoff, J. I. Gersten, and A. Nitzan, *J. Chem. Phys.* 78, 5324 (1983).

SECOND HARMONIC GENERATION OF RETINAL CHROMOPHORES

Abstract

The second harmonic signal from monolayers of retinal and retinal Schiff bases is reported. The results have yielded information on the monolayer structure and demonstrate that retinal and retinal Schiff bases have large second order molecular hyperpolarizabilities with values of 1.4×10^{-28} esu, 1.2×10^{-28} esu, and 2.3×10^{-28} esu for retinal, the unprotonated Schiff base, and the protonated Schiff base, respectively. These values compare well with the known variation in the alteration in the dipole moment of such chromophores upon excitation.

1. Introduction

The initial step in the process of visual excitation is the absorption of light in the chromophore. In all visual pigments, the chromophore is a derivative of retinal (Vitamin A aldehyde). Thus, a detailed study of the excited state properties of this retinylidene chromophore and related molecules is a crucial step in understanding the visual process.

Several spectroscopic techniques[1] have been applied to investigate the photophysical and photochemical properties of the retinylidene chromophore. But few nonlinear optical techniques have been used. Such methods can yield interesting information as has been demonstrated in other system.[2,3] Second harmonic generation (SHG) is the lowest order nonlinear optical process, in which the second order polarizability of a material is responsible for the generation of light at the second harmonic frequency. Due to symmetry consideration, the SHG is forbidden in an isotropic medium in the electric dipole approximation, but allowed at the surface where the inversion symmetry is broken. It was recognized by Y. R. Shen et al.[4] that this attribute can be used to probe adsorbed monolayers at surfaces with high spatial and temporal resolution. Of great importance is the fact that this technique has

been demonstrated to have submonolayer sensitivity[5,6] and recently Th. Rasing et al.[7] have proposed a simple and direct method to measure the second-order molecular polarizabilities of some organic molecules by using the surface second harmonic generation technique directly on a Langmuir-Blodgett trough.

Monolayers based on Langmuir-Blodgett troughs have attracted renewed interest during the last few years[8] because such troughs allow the organization of appropriate molecules in a planned way so that the realization of artificial devices acting at the molecular scale becomes imaginable. The properties of biological membranes can readily be simulated by Langmuir-Blodgett (LB) monolayers. Second harmonic generation has the potential of being used as a direct, *in situ* surface probe of such monolayers. Using this probe, detailed information can be obtained on the physical, chemical and biological properties of these monolayers.

In this paper we apply SHG to compare the second harmonic properties of monolayers of retinal, retinylidene n-butylamine Schiff base (NRB) and protonated NRB (PNRB). The results have yielded new insight into the structure and dipolar properties of these molecules.

2. Experimental Procedures

A Q-switched frequency doubled Nd:YAG laser with a 10Hz repetition rate and 10nsec pulsewidth was used. The Nd:YAG laser was adjusted to give a green 532nm beam of less than 20mW which was focused onto a 3mm

diameter spot on the sample surface after passing through a half-wave plate, a Glan-Thompson laser prism polarizer and a KG-5 color glass filter. The reflected second harmonic signal at a wavelength 266nm was passed through a UG-5 color glass filter which blocked the fundamental at 532nm. The UG-5 filter was followed by a UV Glan-Taylor polarizer and a Schoeffel 0.2m double monochromator. The SH signal was detected by a cooled RCA C31034 photomultiplier and averaged by a boxcar integrator.

All-*trans* retinal purchased from Sigma was dissolved in n-hexane without further purification. High pressure liquid chromatography indicated that the all-*trans* retinal was greater than 95% pure. All-*trans* retinylidene butylamine Schiff base (NRB) was prepared as described before[9]. The molar concentrations of retinal, unprotonated and protonated NRB in methanol solutions were determined by the published extinction coefficients $\varepsilon_{380} = 4.2884 \times 10^4 M^{-1}cm^{-1}$ [10a], $\varepsilon_{365} = 5.23 \times 10^4 M^{-1}cm^{-1}$ and $\varepsilon_{445} = 4.98 \times 10^4 M^{-1}cm^{-1}$ [10b] respectively. The molecules were spread on the surface of deionized distilled pure water subphase at pH 6.4.

The Langmuir trough was made out of teflon. A movable barrier controlled the surface density of molecules and a #40 filter paper with dimension 0.7cm x 1.0cm was attached to a Gould UC-3 force transducer to measure the surface pressure. During detection of the second harmonic signal, the movable barrier was controlled by a stepping motor such that the surface pressure of the film was kept at constant value.

Molecular orientation was determined by using the Heinz's nulling technique[11]. The incident pump beam was arranged to satisfy the following condition:

$$[\ e_{\parallel}(\omega)/e_{\perp}(\omega)\ ]^2 = 2 \qquad 1$$

where $e(\omega)$ is the product of the polarization vector and the Fresnel factor for the pump field in the monolayer[12]. The subscripts denote the components of $e(\omega)$ on or perpendicular to the layer plane. This condition can be met by adjusting the pump beam to have an angle of incidence of 45^0 and a polarization of 35.3^0 away from the incident plane. The molecular orientation was determined by the second harmonic extinction direction, as indicated by the UV polarizer.

Our detection sensitivity was calibrated against the second harmonic intensity from an x-cut quartz plate, observed under the same experimental conditions. The quartz plate was rotated 28.75^0 about the y-axis of the crystal to obtain one of the maxima of the Maker's fringes. The polarizations of the fundamental and second harmonic beams were chosen to be p-polarized relative to the plane of incidence. In this case, the two beams are the extraordinary waves of the quartz crystal. Using the known nonlinear second order susceptibility $d_{11} = 2.4 \times 10^{-9}$esu [13] and the index of refraction of quartz at 532nm and 266nm, we obtained a ratio of [14]

$$I_{p\rightarrow p}(2\omega)/[I_p(\omega)]^2 = 3.96 \times 10^{-26}\ cm^2\ erg^{-1} \qquad 2$$

The potential energy barrier between the water subphase and the NRB monolayer is quite small. This is particularly true for the NRB on an acid (pH 2.8) water subphase. We have observed that the unprotonated NRB molecules leak through the movable barrier on the acid water subphase during the compression stage. In addition, the proton on the Schiff base notrogen of protonated NRB was found to be able to detach from the nitrogen. In order to avoid these problems, the second harmonic intensities from unprotonated and protonated NRB monolayers were compared by using spin-coated monolayers on glass substrates.[15] The monolayers were carefully prepared to make sure that they have the same surface density of molecules. Several steps were taken to prevent the molecules on the glass substrates from isomerization. First, the average power of the pump laser was limited to below 15mW when the spin-coated samples were measured. Second, the data collection time was reduced to 20sec and third, the samples were mounted on a spinning DC motor to minimize the exposure time of molecules to the pumping laser beam.

3. Results and Discussion

Correlation of Mechanical and Structural Properties of Retinal and Schiff Base Monolayers

The molecular structures of all-*trans* retinal and its Schiff bases are shown in Figure 1. The initial characterization of the all-*trans* retinal unprotonated retinylidene n-butylamine Schiff base (NRB) Langmuir-Blodgett films were made by measuring surface pressure/surface area (π-A) isotherms. This allowed the mechanical properties of the films to be assessed. These measurements are shown in Figure 2, where the curve (a) and (b) are for retinal and unprotonated NRB respectively. The limiting areas $A_{\pi \to 0}$ obtained from extrapolation of the linear part to zero pressure,[16] were found to be 58Å^2 for retinal and 69Å^2 for unprotonated NRB. Based on the linear dimensions estimated from space-filling models of retinal, 18Å, these limiting areas suggest the molecular long axes must tilt away from the water subphase surface. This observation is consistent with the results of the molecular orientation measurement, which are shown in Figure 3. The only difference between the chemical structures of retinal and unprotonated NRB is that the oxygen atom in retinal is replaced by a butylamine group (see Figure 1). The additional butyl group will require the NRB molecule to occupy a larger surface area than retinal does under the same surface pressure. However this does not have any appreciable effect on the molecular orientation (see Figure 3). In this measurement the molecular directions of retinal and NRB are studied as a function of

compressing the surface area and increasing the surface pressure. As is seen in this Figure, for each of these molecules at low surface pressure a molecule direction of $\simeq 70^0$ relative to the surface normal is approached whereas at high surface pressure this angle reaches $\simeq 50^0$.

The cross section of the β-ionone ring on a plane perpendicular to the molecular long axis has dimensions of 5.2Å by 7.7Å. If most of the steric interaction among molecules comes from the β-ionone ring, it would be expected that the LB films become closely packed at a surface area of 40Å^2. Indeed from Figure 2, we observe that the isotherms of these two species level-off below 32Å^2. The slight difference of 8Å^2 can be attributed to the dynamic property of the molecules on the water surface. In order to examine the structure of the film, we have measured the second harmonic intensity under different surface pressures. The results are shown in Figure 4. It was observed that the SH p-polarized intensity $I_{s\rightarrow p}$ increase with the surface pressure in a nonlinear fashion. This is understandable by considering that the SH intensity is proportional to the absolute square of the second order molecular hyperpolarizability, β, by a coordinate transformation that depends on the molecular orientation:[4]

$$(\chi^{(2)})_{ijk} = N_s \langle G^{\xi\eta\zeta}_{ijk}(\theta,\phi,\psi)\rangle\beta \qquad 3$$

Here, $\langle G^{\xi\eta\zeta}_{ijk}\rangle$ is the geometric factor specified by the coordinate transformation from the molecular coordinates (ξ,η,ζ) to the lab coordinates (i,j,k), with the Euler angles (θ,ϕ,ψ) describing the molecular orien-

tation and the angular brackets indicating an average over all the molecules. From Figure 3, we found $\langle G_{ijk}^{\xi\eta\zeta} \rangle$ can depend on the surface pressure by way of the molecular orientation. Furthermore, the surface density N_s is not a linear function of the surface pressure as indicated in Figure 2. The SH intensity $I_{p\to p}$ on the other hand monotonically decreases with the surface pressure. It drops to zero at 14 dynes/cm. The second harmonic p-polarized electric field strength $E_{p\to p}(2\omega)$ is obtained in terms of the incident p-polarized field:[17]

$$E_{p\to p}(2\omega) \propto \langle\beta\rangle_{zxx}(\varepsilon_W - \sin^2\alpha)(1 - \frac{2\varepsilon_2}{\varepsilon_1}) + \langle\beta\rangle_{zzz}\sin^2\alpha(\frac{\varepsilon_W}{\varepsilon_1})^2 \quad 4$$

where ω is the angular frequency of the incident radiation, α is the angle of incidence (45^0 in our case), ε_W, ε_1 and ε_2 are the dielectric constants of the water subphase and of the film at ω and 2ω respectively. $\langle\beta\rangle_{zxx}$, $\langle\beta\rangle_{zzz}$ are the two distinct nonvanishing average molecular hyperpolarizability components for the isotropic film considered here. For a rod shape molecule like retinal, the second-order molecular hyperpolarizability tensor is dominated by the one component corresponding to the incident and second-harmonic electric fields lying along the axis of the molecule. If the molecular axes are inclined at an average angle θ to the subphase normal but have a random distribution of azimuthal angle, then

$$\langle\beta\rangle_{zzz} = \beta\cos^3\theta$$
$$\langle\beta\rangle_{zxx} = \frac{1}{2}\beta\sin^2\theta\cos\theta \quad 5$$

The vanishing value of $E_{p\to p}(2\omega)$ implies that the inclination angle of

the retinal molecule has a value of 59°. This is consistent with the molecular orientation measurement by the Heinz's nulling technique (as described above and shown in Figure 3).

We have also observed the relaxation phenomenon of the all-*trans* retinal LB film. The LB film was compressed to have 11 dynes/cm of surface pressure and then was kept at the constant area condition. The time course of the molecular orientation and surface pressure were recorded during the film relaxation. We found that the molecular directions closely follow the surface pressure (see Figure 5). This suggests that the force which keeps the molecules standing up from the water surface mainly comes from the steric interaction between molecules and the same force takes part in generating the surface pressure.

Correlation of Second Harmonic Generation with Dipolar Properties of Retinal and Retinal Schiff Bases

Recent studies of nonlinear second order optical processes in organic molecules have shown that two factors are important for a molecule to have large nonlinear optical response to an external applied field.[18] The first is that molecules must have a highly polarizable π-electron system and the second is that the π-electron system has to be distorted by interaction with strong electron donor and acceptor groups. Although retinal does not have explicit electron donor and acceptor groups, the charge transfer by way of the π-electron system can occur during the electronic excitation $^1B_u \leftarrow S_0$. Quantum-

chemical calculations[19] have demonstrated that there is a dramatic change in charge distribution from the β-ionone ring to the carbonyl group such that the oxygen is more negative in the first excited singlet $\pi\pi^*$ state. Mathies et al. has used an electrochromic technique to monitor the electronic dipole moments of retinal, unprotonated and protonated NRB during the electronic excitation $^1B_u \leftarrow S_0$.[20] Their data confirmed that retinal's condensed-phase dipole moment increases substantially (14.7 Debyes) upon excitation with the unprotonated NRB having slightly less change (10.2 Debyes) in dipole compared to retinal. In protonated NRB, the proton attached to the Schiff base nitrogen encourages the charge-transfer process and therefore increases the dipole moment change to 15.2 Debyes. Charge-transfer of this type should provide a substantial contribution to the second-order molecular hyperpolarizability. A simple two-level model has been used[21] to express this term as:

$$\beta = \frac{3e^2\hbar^2}{2m} \frac{W}{[W^2-(2\hbar\omega)^2][W^2-(\hbar\omega)^2]} f\Delta\mu_{ex} \qquad 6$$

where $\Delta\mu_{ex}$ is the difference between excited- and ground-state dipole moments, f is the oscillator strength of transition, $\hbar\omega$ is the fundamental photon energy, and W is the energy of transition. If the charge-transfer process is the major mechanism in the second-order nonlinear optical response of retinal, unprotonated and protonated NRB, the SH intensities from these three species should show the same increasing tendency from unprotonated NRB to retinal to protonated NRB as seen in the data of Mathies and Stryer.[20] Table I summarizes our SH measurements for these molecules. We have found that the SH intensity from an

unprotonated NRB LB film at a surface pressure of 13 dynes/cm is 70% of the SH intensity observed from a retinal LB film under the same conditions. By correcting for oscillator strength and energy dispersion factors, we have obtained 0.73 for the ratio of the dipole moment changes between unprotonated NRB and retinal, close to the 0.69 value from the data of Mathies and Stryer. The SH signal from protonated NRB film is 3.7 times stronger than that of unprotonated NRB. After the same correction procedure, we have a ratio 0.97 between protonated NRB and retinal whereas the Mathies and Stryer data gives a value of 1.03. The consistency of our data with the work by Mathies and Stryer using the very different Stark shift technique is most encouraging.

By calibrating the SH signal against a thin x-cut quartz plate, the second-order molecular hyperpolarizability of retinal is estimated to be 1.4×10^{-28}esu, which is over two times larger than 2-methyl-4-nitroaniline (β=4.5×10^{-29}esu at 0.83μm). A value of 1.2×10^{-28} esu for unprotonated NRB and 2.3×10^{-28} esu for protonated NRB were found. The large second-order molecular hyperpolarizability that we have measured and the near 55^0 adsorbed direction insure that such molecules are efficient SH generator. Recently A. Gierulski et al.[22] has demonstrated a novel technique to measure the pulsewidth of a subpicosecond laser based on the SH generation from a dye-coated substrate. The time resolution is found to be limited by the transverse relaxation time (T_2) of dye molecules. We have used a temporarily incoherent broadband Stilbene-420 dye laser with 68 femtosecond correlation time to measure the incoherent photon echoes[23] from protonated and unprotonated NRB. Our results show[24] that the T_2 of protonated NRB at 420nm is shorter

than 15fsec. Our experiment suggests that retinal, protonated and unprotonated NRB can be very efficient time-correlation devices for subpicosecond light pulse measurements.

4. Conclusion

In conclusion, we have measured the second harmonic generation of retinal, unprotonated, and protonated retinylidene n-butylamine Schiff bases at air-water and air-glass interfaces. Our data support the conclusions of other workers that the first excited singlet state dipole moments of retinal and its Schiff bases have a major contribution from the charge-transfer process which takes place from the β-ionone ring to the end groups of these molecules. The long-axes of the molecules tilt away from the surface normal by nearly 55°. The second-order molecular hyperpolarizability of protonated NRB is larger than unprotonated NRB and the increment can be explained by the stabilization of the π- electron system provided by the proton which is attached to the Schiff base nitrogen. We believe that this technique could readily be extended to other relevant biological and chemical applications which require the investigation of dipolar and structural relationships between related systems.

The results reported in this paper are currently being extended to determine the light induced alteration of the dipolar characteristic of the retinylidene chromophore in the membrane bound bacteriorhodopsin.[25]

This work was supported partially by U.S. Army Contract No. DAMD17-85C-5136 and a grant from the U.S. Air Force to A.L. and partially by the Director, Office of Energy Research, Office of Basic Energy

Sciences, Materials Sciences Division of the U.S. Department of Energy under Contract No. DE-AC03-76SF00098.

Table I. Comparisons of the second-order molecular hyperpolarizabilities and the dipole moment changes of the first excited $\pi\pi^*$ singlet state for all-*trans* retinal, unprotonated and protonated retinylidene n-butylamine Schiff bases

molecules	surface susceptibility $\chi^{(2)}_{zxx}$ (esu) (N_s=2.5 x 10^{14})	second-order molecular hyperpolarizability β (esu)	excited-stated dipole moment changes (relative to retinal) this work	Mathies's
all-*trans* retinal	6.6 x 10^{-15}	(1.4 ± 0.4) x 10^{-28}	1	1
unprotonated retinylidene n-butylamine Schiff Base (NRB)	5.8 x 10^{-15}	1.2 x 10^{-28}	0.73	0.69
protonated retinylidene n-butylamine Schiff Base (N^+RB-HCl)	1.1 x 10^{-14}	2.3 x 10^{-28}	0.97	1.03

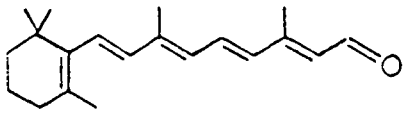

(a) All-trans Retinal

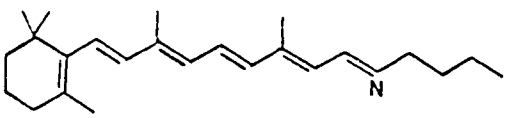

(b) All-trans Retinylidene n-Butylamine Schiff Base (NRB)

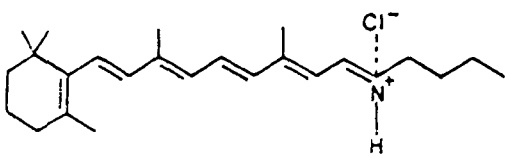

(c) Protonated All-trans Retinylidene n-Butylamine Schiff Base (N^{+}RB-HCl)

XBL 8710-4004

Fig. 1. The chemical structures of (a) all-trans retinal, (b) all-trans retinylidene n-butylamine Schiff base (NRB) and (c) protonated all-trans retinylidene n-butylamine Schiff base (N^{+}RB-HCl).

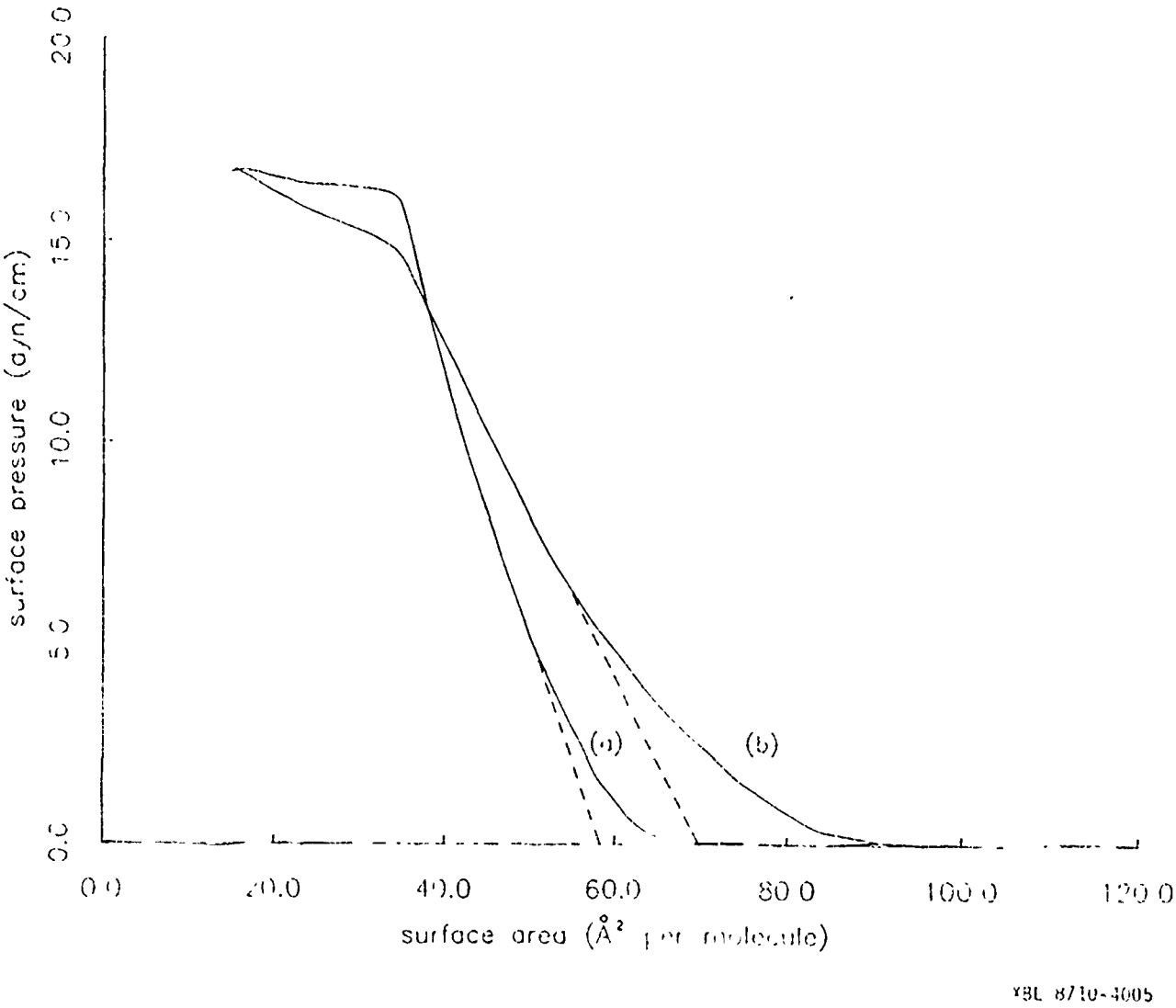

Fig. 2. The surface pressure-surface area (π-A) isotherms of (a) all-trans retinal (b) unprotonated retinylidene n-butylamine Schiff base (NRB) Langmuir-Blodgett monolayers on a pure water subphase. The dashed lines indicate the extrapolations of the linear parts to zero pressure. The limiting areas are 58Å^2 for retinal and 69Å^2 for NRB respectively. The cross point of these two isotherms is at the point where the surface pressure is 13 dynes/cm and the surface area is 38Å^2/molecule.

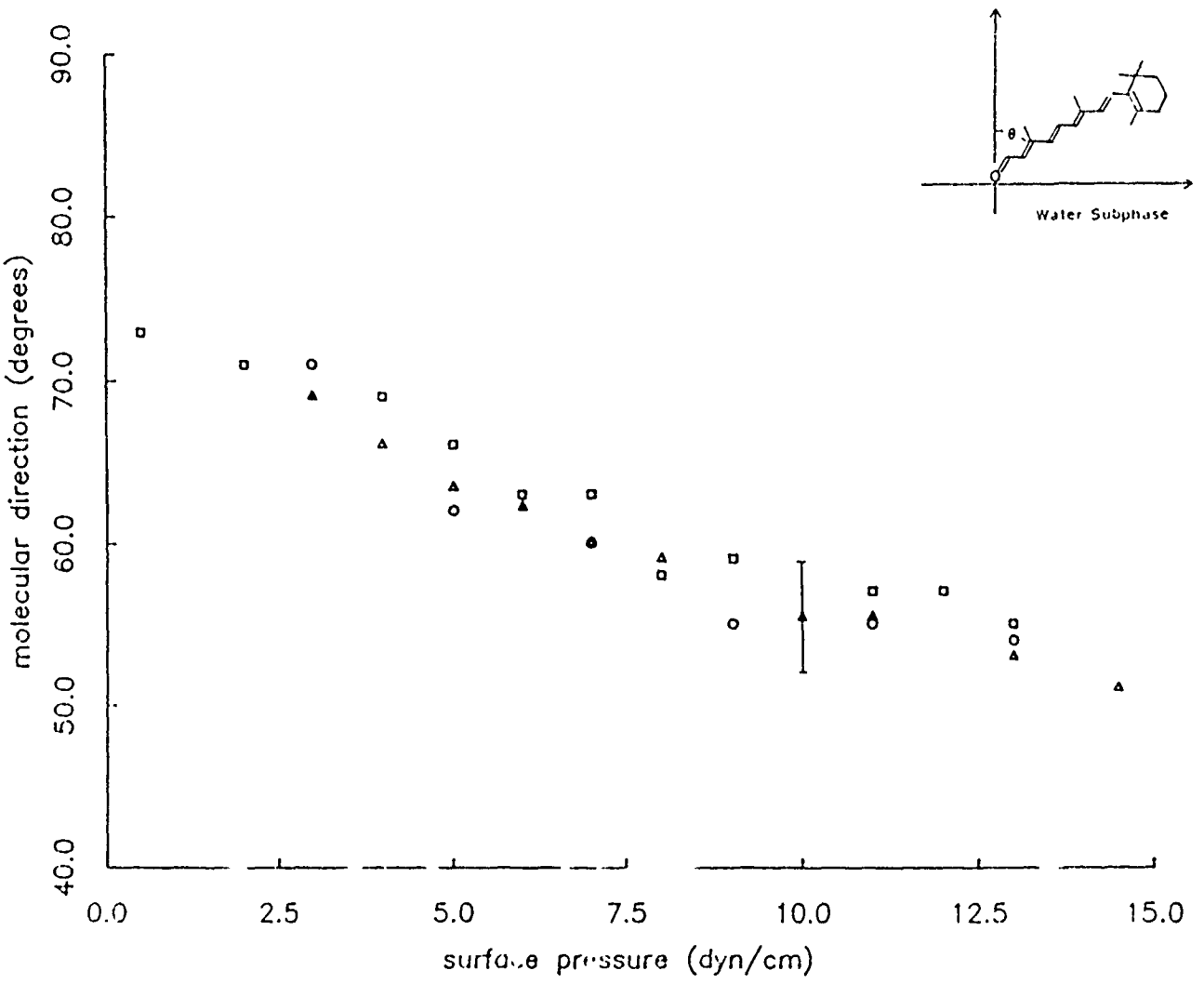

Fig. 3. The molecular orientation at different surface pressures. The open circles and open boxes are for all-trans retinal and retinal Schiff base (NRB) monolayers respectively. The open triangles are for NRB on a 4mM $CdCl_2$ water subphase. The inset figure indicates the orientation parameter that was measured.

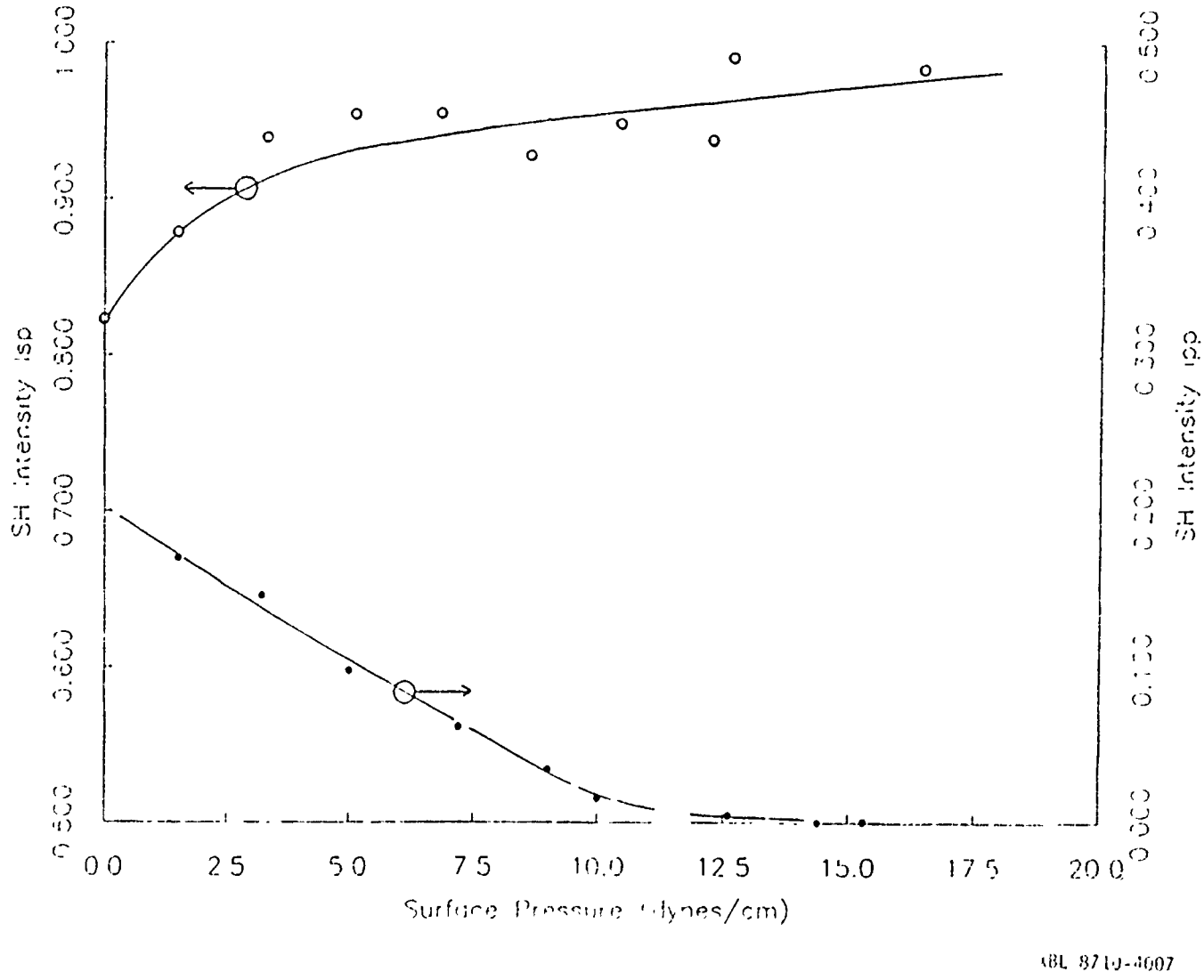

Fig. 4. The second harmonic (SH) intensity of retinal monolayer at different surface pressures. The SH p-polarized intensity with an s-polarized pump beam, $I_{s\to p}$, which is proportional to the absolute square of the second-order susceptibility $\langle B\rangle_{zxz}$ of the molecular monolayer whose surface coincides with the xy-plane, is shown in open circles. The solid circles are for $I_{p\to p}$ SH intensity, which drops to zero when surface pressure is above 14 dynes/cm. The solid lines through the points are only intended to guide the reader.

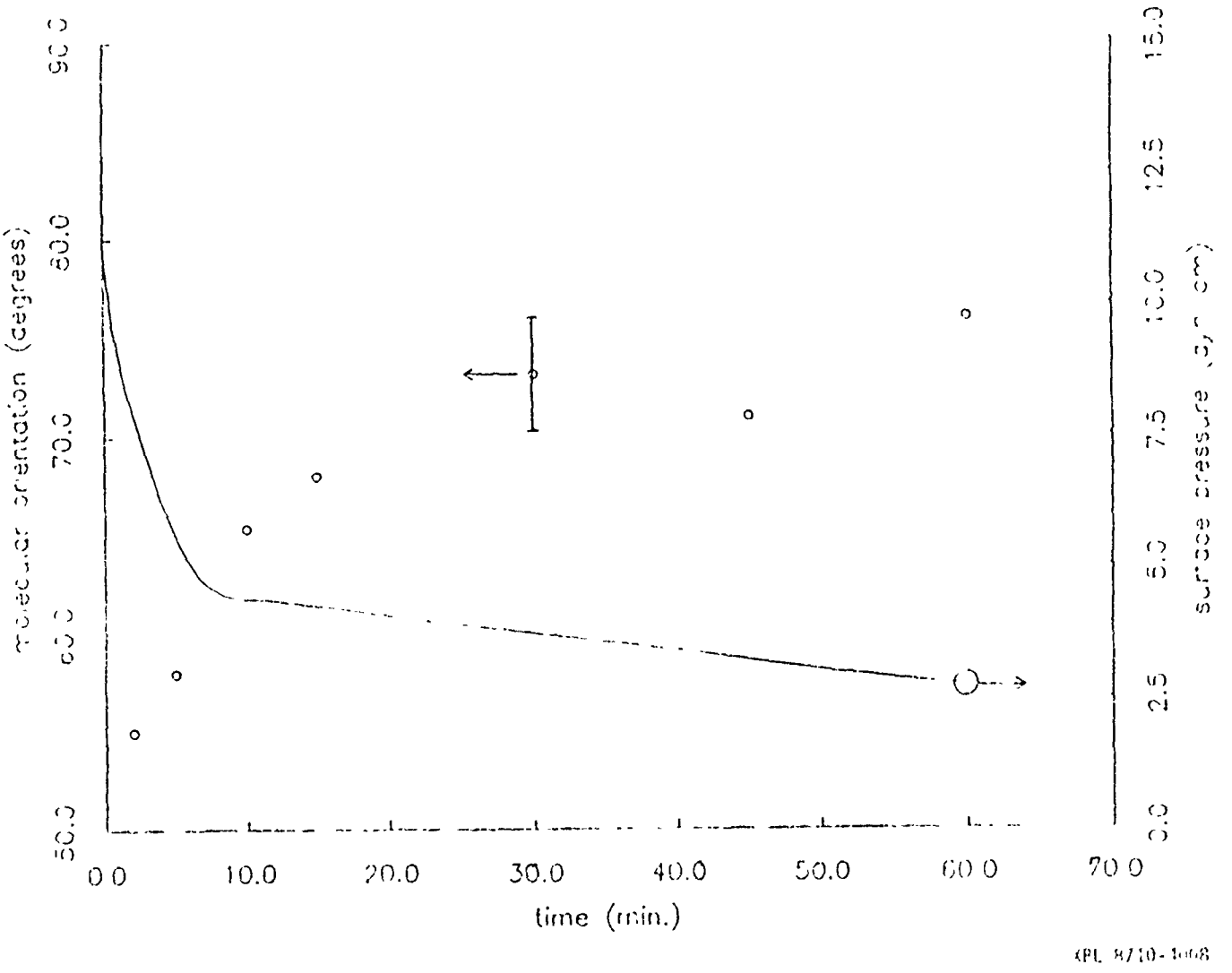

Fig. 5. The relaxation behavior of the molecular orientation (open circles) and surface pressure (solid line) of the all-trans retinal LB monolayer. The LB film was first compressed to 11 dynes/cm and then let it relax under the constant area condition.

References

(1) For review see, Methods in Enzymology, Vol. 88, Part I, ed. L. P. Packer (Academic Press, New York, 1982).

(2) Nestor, J. R.; J. Raman Spectros. 1978, 7, 90.

(3) Levenson, M.D.; Introduction to Nonlinear Laser Spectroscopy (Academic Press, New York, 1982).

(4) Shen, Y. R.; Ann. Rev. Mater. Sci. 1986, 16, 69.

(5) Tom, H. W. K.; Mate, C. M.; Zhu, X. D.; Crowell, J. E.; Heinz, T. F.; Phys. Rev. Lett. 1984, 52, 348.

(6) Tom, H. W. K.; Mate, C. M.; Zhu, X. D.; Crowell, J. E.; Shen, Y. R.; Somorjai, G. A.; Surf. Sci. 1986, 172, 466.

(7) Rasing, Th.; Berkovic, G.; Shen, Y. R.; Grubb, S. G.; Kim, M. W.; Chem. Phys. Lett. 1986, 130, 1.

(8) E.g.: Second International Conference on Langmuir-Blodgett Films, Schenectady, New York, 1985, ed. Zemel, J. N.; Thin Solid Films, 132, 133, 134.

(9) Marcus, M. A.; Lemley, A. T.; Lewis, A.; J. Raman Spectros. 1979, 8, 22.

(10) (a) Becker, R. S.; Freedman, K.; J. Am. Chem. Soc. 1985, 107, 1477.

(b) Becker, R. S.; Freedman, K.; Lenoble, C.; J. Phys. Chem. 1986, 90, 4334.

(11) Heinz, T. F.; Tom, H. W. K.; Shen, Y. R.; Phys. Rev. A 1983, 28, 1983.

(12) Dick, B.; Gierulski, A.; Marowsky, G., Reider, G. A.; Appl. Phys. B 1985, 38, 107.

(13) Miller, R. C.; Appl. Phys. Lett. 1964, 5, 17.

(14) (a) Jerphagnon J.; Kurtz, S. K.; J. Appl. Phys. 1970, 41, 1667.

(b) Miller, R. C.; Phys. Rev. 1963, 131, 95.

(15) Heinz, T. F.; Chen, C. K.; Ricard, D.; Shen, Y. R.; Phys. Rev. Lett. 1982, 48, 478.

(16) Nakahara, H.; Fukuda, K.; Möbius, D.; Kuhn, H.; J. Phys. Chem. 1986, 90, 6144.

(17) Girling, I. R.; Cada, N. A.; Kolinsky, P. V.; Montgomery, C. M.; Electron. Lett. 1985, 21, 169.

(18) Garito, A. F.; Singer, K. D.; Teng, C. C.; in Nonlinear Optical Properties of Organic Materials, ed. Williams, D. J. (ACS, Washington, D.C., 1983).

(19) Birge, R. R.; Hubbard, L. M.; J. Am. Chem. Soc. 1980, 102, 2195.

(20) (a) Mathies, R.; Stryer, L.; Proc. Natl. Acad. Sci. USA 1976, 73, 2169.

(b) Ponder, M.; Mathies, R.; J. Phys. Chem. 1983, 87, 5090.

(c) Davidsson, A.; Johansson, L. B. A.; J. Phys. Chem. 1984, 88, 1094.

(21) Frazier, C. C.; Harrey, M. A.; Cockerham, M. P.; Hand, H. M.; Chauchard, E. A.; Lee, C. H.; J. Phys. Chem. 1986, 90, 5703; Oudar, J. L.; Chemla, D. S.; J. Chem. Phys. 1977, 66, 2664.

(22) Gierulski, A.; Marowsky, G.; Nikolaus, B.; Vorobev, N.; Appl. Phys. B 1985, 36, 133.

(23) Nakatsuka, H.; Tomita, M.; Fujiwara, M.; Asaka, S.; Optics Commun. 1984, 52, 150.

(24) Huang, J.; Lewis, A.; unpublished results.

(25) Rasing, Th., Huang, J.; Lewis, A.; Stehlin, T.; Shen, Y. R.; to be published.